CHALMERS
UNIVERSITY OF TECHNOLOGY

Online Monitoring of Brake Capability For Heavy Vehicles

Master's thesis in Automotive Engineering

Ramprasad Soundhararajan
Prajwal Devegowdana Koppal Chandrashekar

Department of Mechcanics and Maritime Sciences
CHALMERS UNIVERSITY OF TECHNOLOGY
Gothenburg, Sweden 2019

Master's thesis 2019:11

Online Monitoring Of Brake Capability for Heavy Vehicles

Ramprasad Soundhararajan
Prajwal Devegowdana Koppal Chandrashekar

CHALMERS
UNIVERSITY OF TECHNOLOGY

Department of Mechanics and Maritime Sciences
Division of Vehicle Engineering and Autonomous Systems
Chalmers University of Technology
Gothenburg, Sweden 2019

Online Monitoring Of Brake Capability For Heavy Vehicles
Ramprasad Soundhararajan
Prajwal Devegowdana Koppal Chandrashekar

Supervisor: Leon Henderson, Volvo Group Truck Technology
Examiner: Bengt Jacobsson, Chalmers University Of Technology

Master's Thesis 2019:11
Department of Mechanics and Maritime Sciences
Division of Vehicle Engineering and Autonomous Systems
Chalmers University of Technology
SE-412 96 Gothenburg
Telephone +46 31 772 1000

Cover: https://www.volvotrucks.se/content/dam/volvo/volvo-trucks/masters/euro-6/volvo-fmx/media-gallery/2326x1310-media-gallery-volvo-fmx-with-i-shift.jpg

Chalmers Reproservice
Gothenburg, Sweden 2019

Online Monitoring Of Brake Capability For Heavy Vehicles

Ramprasad Soundhararajan
Prajwal Devegowdana Koppal Chandrashekar
Department of Mechanics and Maritime Sciences
Chalmers University of Technology

Abstract

The recent advancement in heavy vehicle brakes involves development of a novel fast-acting electronic brake system. This brake system comprises a slip controller that aids in reducing the stopping distances and tracks longitudinal wheel slip demands accurately during extreme braking manoeuvres. The slip controller and pressure controller relies on the knowledge of the 'brake gain' to calculate the desired brake pressures. The brake gain is defined as a relation between applied brake pressure and received brake torque. Currently the brake gain is assumed to be known and a constant, which is far from true.

In this master thesis an algorithm to measure and estimate the brake gain on-line has been developed and evaluated. The developed estimator captures the variation of the brake gain with brake fade and actuator geometry. A temperature model is developed to estimate disc temperature based on the total braking energy at each braking event. The predicted brake disc temperature is used to estimate the disc-pad interface friction coefficient. Further this information is used to monitor the brake capability. The developed estimator shows that the estimations converge to the reference.

Keywords: Temperature estimation, Brake friction coefficient estimation, Brake gain, Slip controller.

Acknowledgements

The thesis work was carried out at Brake & Suspension Control System, Volvo Groups Truck Technology. Foremost, we would like to express our deep sense of gratitude to our supervisor Leon Henderson at Volvo Trucks and our examiner Bengt Jacobson at Chalmers University. Their constant guidance and support helped us steer our thesis work in the right direction.

Since our work demanded the availability of Volvo brake test data and reports, we thank Anders Vikstrom, Lars Svensson and Martin Linde for assisting in acquiring them in a timely manner. We also thank Martin Petersson for inputs and suggestions related to brake friction in the initial stages of the thesis.

We thank Edo Denth from Haldex AB for inviting us to their brake dyno facility and also for being a great guide during the visit. We further thank him for providing us with test data which greatly helped us to verify and validate our thesis work.

We take this opportunity to also thank Zhetong Mo, Eddy Iciragiye, Arjun Venkataraman, Karthik Ramanan and Yusuf Talha for the thoughtful discussions during the lunch at Volvo Trucks.

Last but not the least, we are indebted to our family and friends for their sacrifice and support throughout our entire education without whom this would not have been possible.

Ramprasad Soundhararajan
Prajwal Devegowdana Koppal Chandrashekar
Gothenburg, 2019

Contents

List of Symbols

F_{xmax}	Maximum available braking force [N]
μ	Coefficient of friction between road and tyre [-]
F_z	Normal force acting on the wheel [N]
λ	Longitudinal slip [-]
v_x	Longitudinal velocity $[m/s]$
ω	Wheel angular velocity [rad/s]
T_B	Brake torque [N/m]
A_c	Effective force-area of the chamber diaphragm $[m^2]$
q_c	Lever ratio in the caliper [-]
μ_{br}	Coefficient of friction between brake disc and pads [-]
r_{br}	Effective radius of the brake pads on the disc [m]
P_c	Pressure in the brake chamber [bar]
G	Brake gain [-]
σ	Heat partition coefficient [-]
ξ	Thermal effusivity $[J/(m^2 s^{\frac{1}{1}} 2K)]$
ξ_d	Thermal effusivity of disc $[J/(m^2 s^{\frac{1}{1}} 2K)]$
ξ_p	Thermal effusivity pad $[J/(m^2 s^{\frac{1}{2}} K)]$
S_d	Frictional contact surfaces of disc $[m^2]$
S_p	Frictional contact surfaces of pad $[m^2]$
k	Thermal conductivity [W/mK]
ρ	Density $[kg/m^3]$
C	Thermal capacity [J/K]
c_p	Specific heat [J/kgK]
m_{disc}	Mass of the disc [Kg]
$\dot{Q}_{in}$	Rate of heat generation [W]
$\dot{Q}_{out}$	Rate of heat dissipation [W]
$\dot{Q}_{rad,pad}$	Rate of radiative heat generated [W]
$\dot{Q}_{conv}$	Rate of convective heat generated [W]

h	Heat transfer coefficient $[W/m^2K]$
A_s	Convective heat surface area $[m^2]$
T	Temperature $[DegreeC]$
T_c	Brake chamber temperature $[DegreeC]$
T_{amb}	Ambient temperature [Degree C]
b	The cooling coefficient [1/s]
ϵ	Emissivity [J/kgs]
σ_{SB}	Stefan-Boltzmann constant $[W/m^2K^4]$
h_{rad}	Radiative heat transfer coefficient $[W/m^2K]$
q_c	Lever ratio [-]
s_s	First order sliding surface [-]
λ_{ref}	Reference slip [-]
R_r	Wheel rolling radius [m]
r_b	Effective brake radius [m]
a_x	Longitudinal acceleration $[m/s^2]$
K_{BG}	Brake gain [-]
k_s	tune-able controller gains [-]
δ	tune-able controller gains [-]
Φ	tune-able controller gains [-]
R_{MS}	Mark Space Ratio [-]
P_{dem}	Pressure demand [bar]
$\dot{m}$	Mass flow rate [kg/s]
V_c	Chamber volume $[m^3]$
R	Specific gas constant for air [J/KgK]
α	Ratio of specific heats [-]
B_i	Biot number [-]
r_0	Disc radius [m]
K	Conductive heat transfer coefficient $[W/m^2K]$

1
Introduction

1.1 Project Background

Heavy vehicles (such as trucks and buses) operate an electronically controlled, pneumatically actuated braking system. This type of system is commonly known as an electronic brake system (EBS). Recent work by Cambridge University, Haldex Brake Products, Volvo Trucks, and Chalmers University has resulted in the development of a novel fast-acting EBS that enables stopping distances to be reduced by up to 17% in low friction conditions.

1.2 Problem motivating the project

A slip controller has been developed utilizing the control bandwidth of the FABVs that is able to accurately track longitudinal wheel slip demands during extreme braking manoeuvres. The slip controller relies on the knowledge of the 'brake gain' (ratio between brake torque and brake pressure) to calculate the desired brake pressures. In the current slip controller implementation, calibration braking tests must be used to calculate fixed brake gain values offline, prior to 'turning on' the slip controller. An on-line brake gain estimation algorithm is needed so that this calibration can be carried out automatically during normal driving. Brake temperature and pad wear should be taken into account to correctly capture the effects of brake fade and actuator geometry changes respectively. The estimated brake gain can also be combined with measurements of the available pneumatic supply pressure to calculate the total available 'brake capability' for a given wheel –this capability information can be used by advanced driver assistance (ADAS) functions to estimate the maximum deceleration that can be achieved by the vehicle.

1.3 Objective

The project objectives are:

- Brake gain and brake capability estimators are to be developed in Simulink using Volvo Trucks' existing vehicle dynamics simulation environment (VTM)
- The developed functions is designed for being hosted by each individual wheel brake module, which has a certain and limited signal interface to the vehicle.
- The estimation routines will be tuned using real test data.

1.4 Deliverables

- Simulation model of disc-braked heavy vehicle (based on Volvo's VTM toolbox) suitable for the development of brake gain and brake capability estimation routines.
- Simulink-based brake temperature and brake gain estimation routines.
- C-code based brake gain and brake capability estimation functions, for implementation in an embedded micro-controller (Autocode generation will be used to generate C-code from Simulink models).

1.5 Limitations

The truck used in this thesis project is the Volvo 8x4 FMX Tridem with tag axle. The development of the brake gain estimator is limited to ventilated disc and pad of this truck. The estimator can be adapted to other trucks by tuning various constants based on real test data. The estimator is based on thermal modelling approach to predict the brake gain and no other methods will be investigated. The friction model does not consider variation in friction due to normal load. The models have also been developed by using test data from straight line braking. Also, influences of external environment such as changing weather conditions has not been studied. Due to limited availability of test vehicle, online calibration was not performed.

1.6 Approach

Although, the brake gain depends on various parameters [12]. The scope of this thesis is limited to temperature, wear and vehicle speed. A thermal model based estimator is developed in Simulink/Matlab with the help of test results from winter tests. The estimator will capture the temperature through this thermal model. The effects of temperature and sliding velocity on coefficient of friction is predicted using a mathematical model fitted to real test data. The brake gain will then be combined with the available supply pressure to determine the maximum brake capability for the wheel. The estimator is further extended to predict the feasible duration of braking before brake fading occurs. The final algorithms will be implemented in the FABVs'micro-processor (using Autocode generation) and tested on-vehicle.

2
Literature Review

Heavy goods vehicles(HGV) are vehicles with gross combination weight above 3500kg. HGV's have been major cause for road fatalities. One major cause of this is poorer braking performance compared to passenger cars. This is due to lower friction associated with truck tires (which are harder and are designed for longer life) and decreased efficiency of brake design themselves [1]. Through technological advancements the number of fatalities in accidents involving HGVs fell by nearly 50% between 2006 and 2015, the percentage of fatalities in accidents involving HGVs did not decrease considerably [2]. Study by Volvo Trucks Accident Research Team(VRT) showed that frontal collision with cars contributes upto 55% of all the accidents involving HGV's [3]. High speeds and differences in mass and geometry between the vehicles lead to high deformation of the car resulting in higher fatalities of car occupants.

Braking can be defined as the process of reducing a vehicle to a lower speed or bringing it to, and keeping it at a complete stop. To achieve this, friction brakes have been long used dating back to 19th century. Friction brakes do so by converting the kinetic energy of the vehicle into heat energy through friction. Other braking systems such as engine braking and retarders exist but are beyond the scope of this thesis [5]. A measure of braking performance is the braking distance i.e the distance travelled during the braking event. During harsh braking events, the braking performance can be severely affected by wheel lockups. A wheel lock up occurs when the applied braking force is much higher than the maximum available, given by the equation 2.1. Many strategies have been implemented to avoid wheel lock ups and improve braking performance which will be discussed in the following section.

$$F_{xmax} = \mu F_z \tag{2.1}$$

Where F_{xmax}, μ, F_z are maximum available braking force, coefficient of friction between road and tyre and normal force acting on the wheel respectively.

2.1 Braking Strategies

Antilock Braking System (ABS) is one of the most widely used brake control strategies. ABS has been made mandatory for all trucks manufactured on or after March 1, 1997 [6]. ABS prevents the wheels from locking by maintaining a vehicle state called longitudinal slip above a certain value typically below 15% or 20% using friction brakes as actuators [8]. Slip (λ) can be defined as:

$$\lambda = \frac{v_x - R_r\omega}{v_x} \tag{2.2}$$

Where R_r,ω and v_x are the rolling radius, wheel angular velocity and longitudinal velocity respectively. The variation of friction for different slips (here called the slip slope curve) and functioning of ABS is shown in figure 2.1.

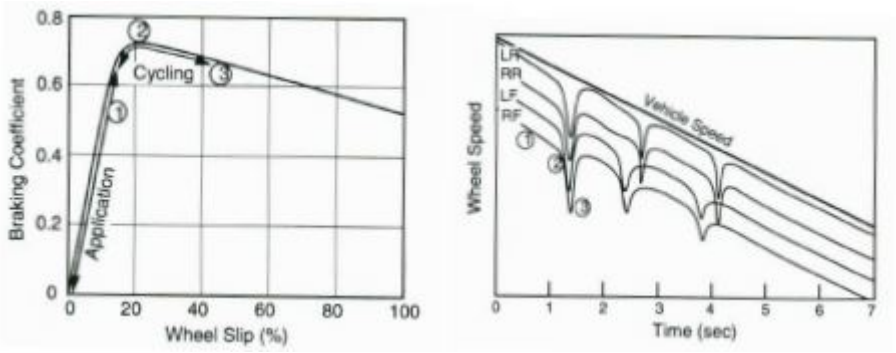

Figure 2.1: Variation of friction coefficient with slip slope curve to the left and ABS control sequence to the right [7]

The slip slope curve can be split into two regions: stable and unstable. The stable region occurs to the left of the peak (point 2) in the slip slope curve where an increase in slip corresponds to an increase in available friction. Conversely, the region to the right of the peak is defined the unstable region. During the brake application, the wheel speed decreases continuously causing an increase in slip represented by point 1 in the figure 2.1. Beyond the peak (point 2), due to reduced available friction, the wheel speed decreases sharply (point 3) indicating possible wheel lock up. Once ABS predicts such a wheel lock up, it release the brake pressure momentarily such that the wheel speed increases again. As a result, the slip decreases resulting in higher available friction. This process is known as ABS cycling.

Although ABS provides a solution that avoids wheel lock up, the ABS cycling causes the wheel slip to vary over a long range as can be seen in figure 2.1. As a result, the maximum available friction and hence, braking force is not completely utilized throughout resulting in lower braking performance.

Alternative solution such as the 'wheel slip control' have been developed to address this issue. The slip controller maintains the wheel slip at a desired value of slip-slope curve by controlling the applied brake torque. The peak value depends on the tyre-force characteristics. Studies have shown that the wheel slip control outperforms ABS by 17% in terms of braking distances [12]. A detailed explanation of the wheel slip control is taken up in section 2.8.

2.2 Volvo Brake System

Unlike in cars where hydraulic pressure is used for control and actuation of friction brake systems, compressed air is used in trucks for actuation. Air brake systems tolerate leakage and provide ease of implementation. The device that converts the compressed air pressure to mechanical force is called the brake actuators. Disc brake and drum brakes are most commonly used in heavy vehicles. Disc brakes have better performance, easier to maintain and have better heat dissipation properties compared to drum brakes [46]. Hence, disc will be the focus in this thesis. In combination with the brake chambers, they form the brake system at the wheel end. A conventional air brake system is depicted in figure 2.2. The brake pressure pushes the push rod against the lever creating mechanical advantage. The lever then applies a force on the bridge. The design of the lever adds further to the mechanical advantage. This force is then applied both on the inner and outer brake pads. The friction material of the pads grips the disc giving rise to the desired retardation by converting the kinetic energy of the vehicle to heat energy.

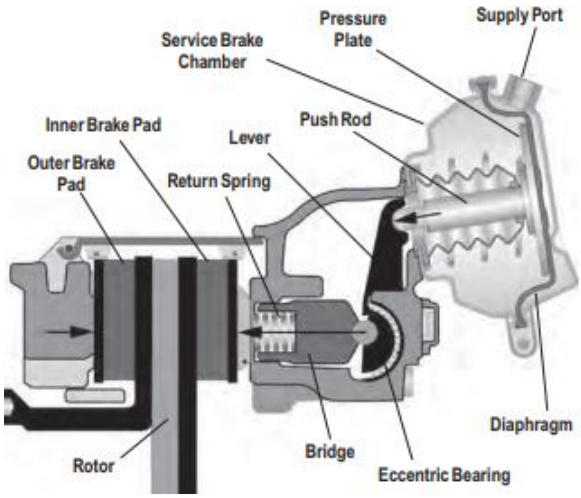

Figure 2.2: Cut away view of an air disc brake [4]

Earlier pneumatic brake systems have slow responses due to pressure development through long pipe lengths in brake chambers. These delays have been drastically reduced through use of electronic communication. Today the Volvo trucks are equipped with Knorr Bremse Electronic Braking System. The electronic actuation helps in faster brake responses which in turn reduces braking distances. Other benefits of the EBS include increased braking comfort, improved brake wear and easier maintenance [9].
Figure 2.3 shows the schematic representation of the EBS-5.

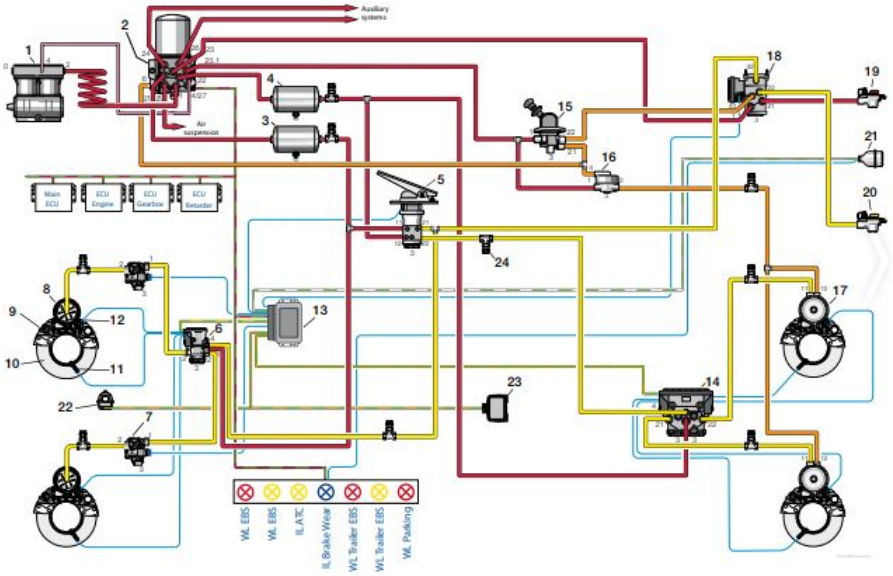

Figure 2.3: A schematic representation of the EBS-5 [10]

As the name suggests, the EBS converts the brake demand/pedal position from the driver to an electronic signal. This signal is then relayed to the main ECU which determines the amount of brake pressure to be applied to achieve the desired vehicle deceleration, while preventing wheel lock (using a low level ABS controller). EBS have been shown to reduce stopping distances by 10% relative to a conventional HGV brake system where purely pneumatic signals are used [11].

Various research and development have been done on actuators and valves to improve braking further. These research focus on replacing the pneumatic brake actuators with electrical components. Haldex Brake Products Ltd have produced a prototype actuator for HGV's and along with wheel slip controller have shown upto 24% reduction in stopping distances [13]. Researchers at Cambridge Vehicle Dynamics Consortium (CVDC) have developed a bi-stable high speed pneumatic valve for use in brake actuator. It consists of a cantilevered steel flexure between two permanent magnets as shown in figure 3.2. The flexure alternates between the two states which can be controlled by electrical pulses with a switching speed of 3ms.

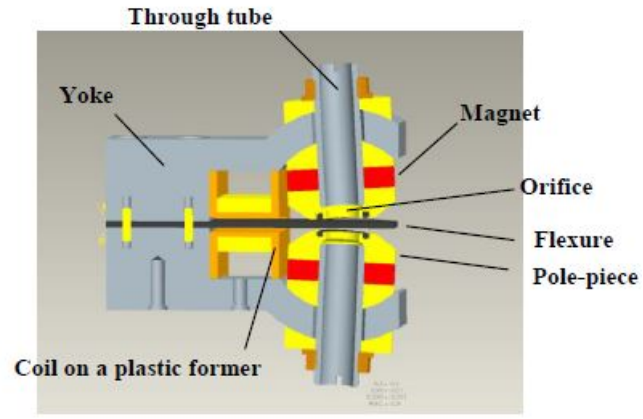

Figure 2.4: Cross section view of the bi-stable valve [12]

2.3 Brake Gain

As seen in the previous section, the brake torque is related to brake pressure. The relationship between brake torque (T_B) and pressure in the brake chamber (P_c) for disc brakes can be defined as:

$$T_B = 2A_c q_c \mu_{br} r_{br} P_c \tag{2.3}$$

Where:

- P_c: Pressure in the brake chamber
- A_c: Effective force-area of the chamber diaphragm
- μ_{br}: Coefficient of friction between brake disc and pads
- r_{br}: Effective radius of the brake pads on the disc
- q_c: Lever ratio in the caliper

The term $2A_c q_c \mu_{br} r_{br}$ is defined as the 'brake gain'(G) [12]. The return spring force is small and hence neglected.

In [12], [13], previous studies of slip control braking performance brake gain was a predefined constant and same for all the wheels i.e the difference in braking behaviour of different axles is neglected. The approximate value of the brake gain (G) was determined using a rolling road dynamometer which allows us to measure the braking force on individual axles for a given brake pressure. A linear fit between chamber pressure (P_c) and braking force (F_x) gives the average brake gain used in [13].

In reality, however, the assumption that the brake gain remains constant throughout the lifespan of the brake is not true. Various factors such as temperature, wear or oil/dirt on the pad affects the brake gain. Also, the instantaneous change in friction due to instantaneous temperature of disc and rotor, as well as their sliding velocity affect the brake gain during the braking event. It is found that brake gain can vary up to $\pm 50\%$ during its usage [14]. Miller [12] has shown that brake gain appears

in the main slip control equation and hence, variation in brake gain affects the performance of the slip controller.
Although immense studies and research have been done to develop new braking technology, there is lack of studies and research for online brake gain estimation. In [12], an algorithm is presented to estimate brake gain using recursive least squares on brake force, determined from pulse braking on each wheel. Acceptable results were obtained, however,the estimator was not consistent through multiple runs.
In [14], recursive least squares method with bounded-forgetting factor is used to estimate the brake gain in real time however the details of the estimator were skipped.
In [15], the brake gain is estimated according to the mapped performance test values of parameters; speed, pad temperature and brake pressure. Since the map was created for a specific truck based on actual tests,the maps are not production feasible. The authors considered temperature of brake pads which are quite different from the actual disc-pad interface temperature. The results presented were not consistent.

2.4 Thermodynamics

During braking, kinetic and potential energy of the vehicle is converted into heat energy due to sliding contact friction of brake disc and pad. This influences wear and frictional characteristics in brake systems and the rate of heat generation is equal to the frictional power [17]. The frictional heat at the disc and pads contact induces high temperature and when the temperature exceeds the critical value, it results in undesirable effects such as brake fade, premature wear, bearing failure, thermal cracks, thermal elasticity and instability [18].
The fraction of generated heat during braking duration absorbed by disc can be calculated [17],

$$\sigma = \frac{\xi_d S_d}{\xi_d S_d + \xi_p S_p} \tag{2.4}$$

Where $\xi_d, \xi_p \& S_d, S_p$ are the thermal effusivity and frictional contact surfaces of disc and pad respectively. Thermal effusivity is defined as:

$$\xi = \sqrt{k\rho C} \tag{2.5}$$

where k, ρ & C are the thermal conductivity, density and thermal capacity respectively. The temperature increase due to heat is given by

$$c_p m_{disc} \frac{dT}{dt} = (\dot{Q}_{in} - \dot{Q}_{out}) \tag{2.6}$$

m,c_p,Q_{in},Q_{out} are the mass of the disc/pad, specific heat of the disk/pad and the rate of heat generation and heat dissipation respectively.

c_p is temperature dependent. A linear relationship between material specific heat and temperature can be derived through a linear regression fit to the brake cooling data [17]. [31] presented a table of c_p for gray iron determined from experimental data, for a range of 25 to 700 degree Celsius.

Thickness: 1.510 mm / Density: 7.169 g/cm³

Temperature /℃	Thermal Diffusivity /mm²/s	Specific Heat /J/(g·K)	Thermal Conductivity /W/(m·K)
25	15.561	0.420	46.854
101	13.556	0.453	44.024
200	11.784	0.494	41.733
300	10.336	0.527	39.050
401	9.114	0.569	37.177
501	7.976	0.632	36.138
601	6.794	0.708	34.484
701	5.344	0.844	32.335

Figure 2.5: Temperature dependent heat capacity for gray iron [31]

[20] derived a linear function for $c_p(T)$ using the above data samples as

$$c_p(T) = 0.0005T + 0.46 \tag{2.7}$$

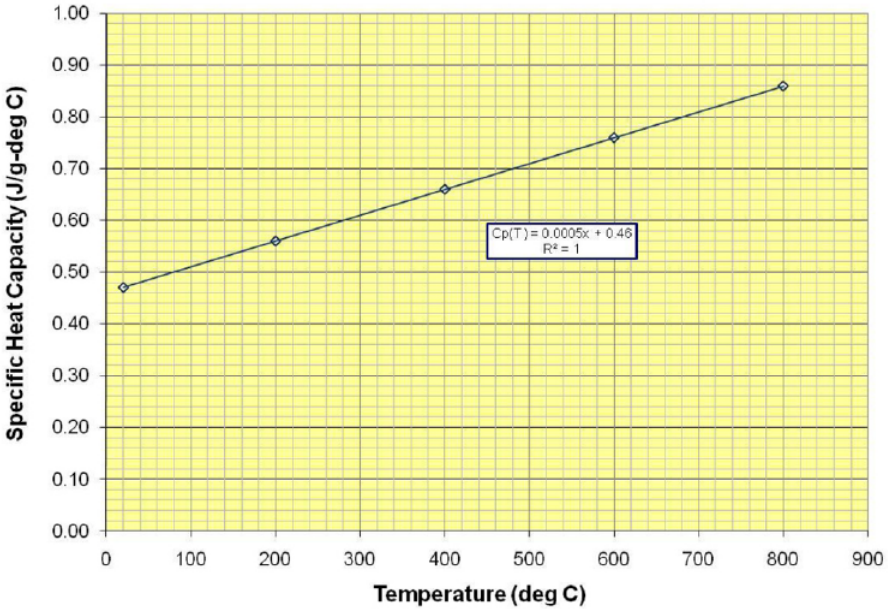

Figure 2.6: Brake rotor gray iron specific heat capacity versus temperature [20]

2.4.1 Heat generation

$\dot{Q}_{in}$ is the heat generation rate at the brake pad-disc interface, during braking. $\dot{Q}_{in}$ is modelled using the following relation [17]:

$$\dot{Q}_{in} = T_B \omega \tag{2.8}$$

where T_B, ω are the braking torque and wheel speed respectively.

A heat partition coefficient (σ) is multiplied with the above equation while modelling heat generation for disc and $(1 - \sigma)$ for pad. The major source of heat flux to the disc is from the conduction of friction heat generated during braking and the major heat source to the brake pad is the radiation from the disc. The amount of radiation absorbed by the pad from the disc is $\dot{Q}_{rad,pad}$ multiplied by a view factor [36].

2.4.2 Heat dissipation

The frictional heat is conducted into the hub, pad and rest of the heat is stored within the disc rotor. The cooling happens exponentially through the phenomena of radiation and convection. At low temperatures, cooling from convection has major contribution compared to the radiation [30].

2.4.2.1 Convection Heat Transfer

The convective heat transfer is modelled using newtons law of cooling,

$$\dot{Q}_{conv} = hA_s(T - T_{amb}) \tag{2.9}$$

The active convective heat surface area A_s is hard to determine because of the complex geometry of the disc. The convective heat transfer coefficient h varies according to the location, vehicle velocity and other factors. The uncertainty in modeling the temperature using the convective heat transfer coefficient h may be as big as 10-30% and is adjusted according to test data [19]. Although various methods can be used to obtain approximate convective heat transfer coefficient such as used in [18] and [22], due to availability of appropriate data the following method was used in this thesis.

The product of h and A_s could be parametrized together to simplify the modeling further [20],

$$-\frac{hA_s}{mc_p}(T - T_{amb}) = \frac{dT}{dt} \tag{2.10}$$

assuming constant c_p the solution to the above differential equation,

$$T(t) - T_{amb} = e^{-bt}(T - T_{amb}) \tag{2.11}$$

$$b = \frac{hA_s}{mc_p} \tag{2.12}$$

Where b is the cooling coefficient and depends linearly on vehicle velocity [32].
In [20], a linear function is setup between the cooling coefficient of the disc and the vehicle velocity.

2.4.2.2 Radiation Heat Transfer

The radiation heat transfer is significant at high temperatures and in low temperatures nearly 5% of dissipation occurs due to radiation [30]. It is modelled from Stefan-Boltzman equation, which predicts a substantial increase of radiative heat dissipation at elevated temperatures:

$$\dot{Q}_{rad} = \epsilon\sigma A_s(T^4 - T_{amb}^4) \tag{2.13}$$

where, A_s, ϵ and σ are the area affected by radiation, the emissivity and the Stefan-Boltzmann constant respectively. The difficult part of radiation heat transfer modelling and analysis relates to the value of emissivity. The material, the condition of the surface and its temperature all influence the value of emissivity. Equation 2.13 is rewritten:

$$\dot{Q}_{rad} = h_{rad}A_s(T - T_{amb}) \tag{2.14}$$

Where h_{rad}, the radiative heat transfer coefficient is defined as [32]:

$$h_{rad} = \epsilon\sigma(T^2 + T_{amb}^2)(T + T_{amb}) \tag{2.15}$$

The variation of h_{rad} with temperature for ϵ average value of 0.55 is as shown in Figure 2.7 [33].

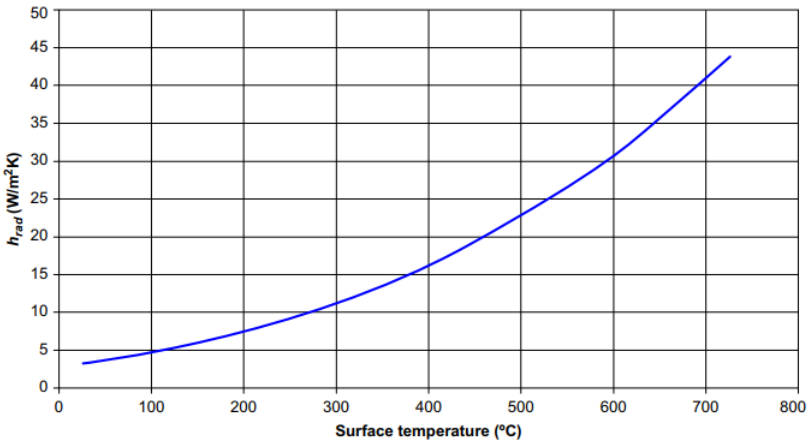

Figure 2.7: Radiative Heat Transfer Coefficient h_{rad} increase with surface temperature for emissivity 0.55 [33]

The heat transfer due to convection and radiation are added together giving $\dot{Q}_{out}$.

$$\dot{Q}_{out} = \dot{Q}_{conv} + \dot{Q}_{rad} \tag{2.16}$$

Equation 2.6 is then integrated to determine the temperature.

2.5 Wear

The contact between the disc and the brake pad´s polymer matrix generate wear particles.The wear and frictional behavior of these material pairs is complex, and is characterized by non-steady state high-temperature and high-pressure processes. Wear is usually characterized with wear rate. Wear rate is one of the important parameters characterizing the performance of friction material. Excessive wear rate results in premature failure of friction material [23]. The wear of friction material depends on factors such as braking pressure, sliding velocity and temperature [24]. The contact pressure of brake disc-pad is a time dependent function of interaction between thermal expansion and wear, where the thermal expansion tends to localize the contact, and wear increases the contact area [27]. In [26], the pad wear properties are investigated for different initial velocities and temperatures. Higher initial braking velocities results in higher temperatures. Pad wear varies linearly with the work done by a brake upto a certain brake temperature and increases rapidly for brake temperatures greater than approximately 320 degrees celsius resulting in tapered pad wear [23] [28].

[29] studied the effect of wear on friction coefficient for different pad composition. The results as shown in Figure 2.8 indicates that for a given particular pad composition the friction coefficient μ stabilizes to an average value. Hence the friction coefficient remains unchanged with wear.

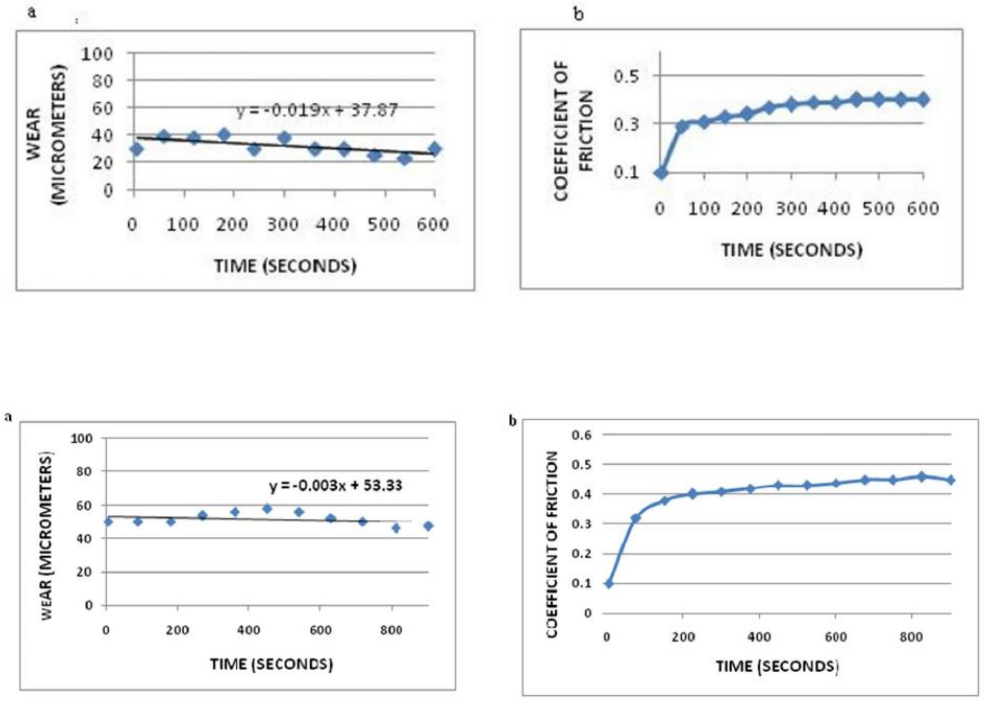

Figure 2.8: Different brake pad composition, (a) Wear vs time (b) Coefficient of friction v/s time [29].

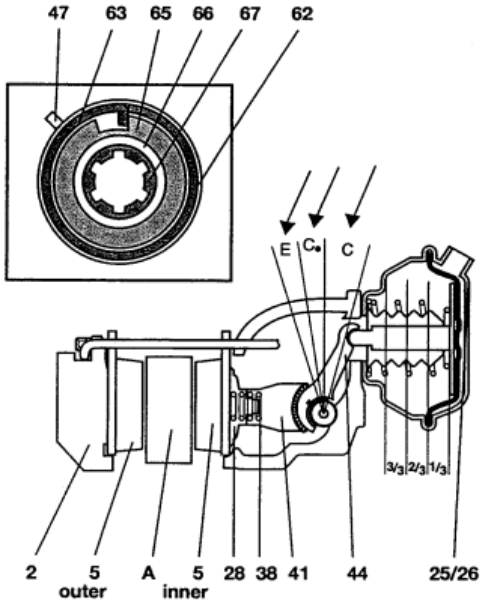

Figure 2.9: Haldex Disc Brake [45].

Most of the modern trucks are equipped with pad wear signals and pad wear compensator mechanism. Pad wear signal provides the prevailing thickness of pad in percentage. So pad wear modelling was excluded. Pad wear mechanism measures the clearance between the pad & disc and in case of excess hub rotation (67) actuates a synchronized bevel gear drive for the twin adjustment screws incorporated in the push bar (41), which then restore the correct clearance between the pads and disc [45]. Hence the effect of wear on brake gain is neglected.

2.6 Lever ratio

The heat generated while braking at the disc-pad interface is conducted through the back-plate to the braking mechanism. This results in higher temperature affecting the efficiency and performance of the mechanism. Apart from friction coefficient, the brake gain depends on lever ratio q_c (from Eq.2.3). From the Figure 4.15, the external and internal radii of the lever (44) is eccentric to force the lever to move axially, resulting in a mechanical advantage. The lever ratio is defined as the ratio of lever length to the eccentricity. With the stroke the lever rotates making an angle thereby changing the ratio. Lever ratio q_c is considered to be constant value 10. But from the brake dynamometer test data, it is observed that at high temperature the stroke is longer for identical brake torque output resulting in the varying lever ratio [44]. This led to close investigation on the effect of varying lever ratio on brake gain.

2.7 Thermal Modelling Approaches

The four different modeling approaches for the thermal analyses of disc brakes [30]:

- A lumped parameter (zero-dimensional) model predicts transient bulk disc temperatures.
- A one-dimensional model provides peak surface as well as bulk temperatures.
- A two-dimensional steady-state model of the entire brake system predicts plateau temperatures during a multistop driving schedule.
- A three-dimensional complex transient model to obtain detailed local disc temperature distributions for any stopping sequence.

1D models are typically used to determine peak operating temperature of the disc, required for the disc design. [30] applied the Finite difference Method and Finite Element Method to 2D and 3D modeling, but due to long computation time they cannot be used for real time estimation.

2.8 Volvo Transportation Model(VTM)

Volvo Transportation Model is a simulink based toolbox used at Volvo GTT for vehicle dynamics related simulation and development. For this thesis, a 8X4 (8 wheels, 4 driven) truck is used to study the braking performance. In our case, the 4^{th} axle also called the tag axle is lifted. The VTM architecture used in this thesis is shown in the figure 2.10.

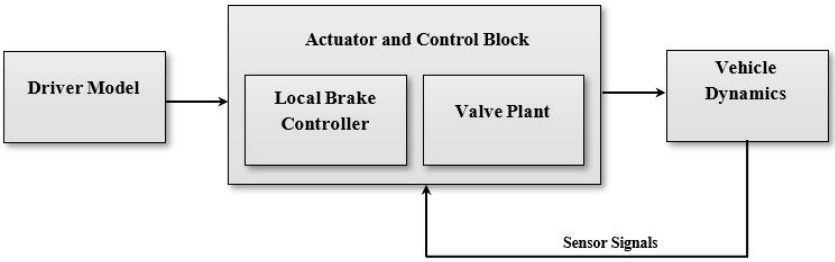

Figure 2.10: VTM architecture

VTM is made up of three major components:

- Driver Model: The driver input such as steering angle, reference vehicle speed, brake torque, etc., is modelled. In this thesis, 80kmph is chosen to be the reference vehicle speed.
- Actuator and Control Block: Individual local brake controller and valve plants are defined for individual wheel inside this block. A schematic representation of the individual brake controller and valve plant combination is shown in figure 2.11.
- Vehicle Dynamics: The truck is modelled as three masses (Chassis front, Chassis rear & cab) with pacejka tire model including 28 parameters. Each axle is also modelled as a separate mass.

A detailed explanation of VTM can be found in [16]. For the convenience of the reader, however, the actuators and control block is discussed briefly here. A schematic representation of the actuators and control block is as shown below:

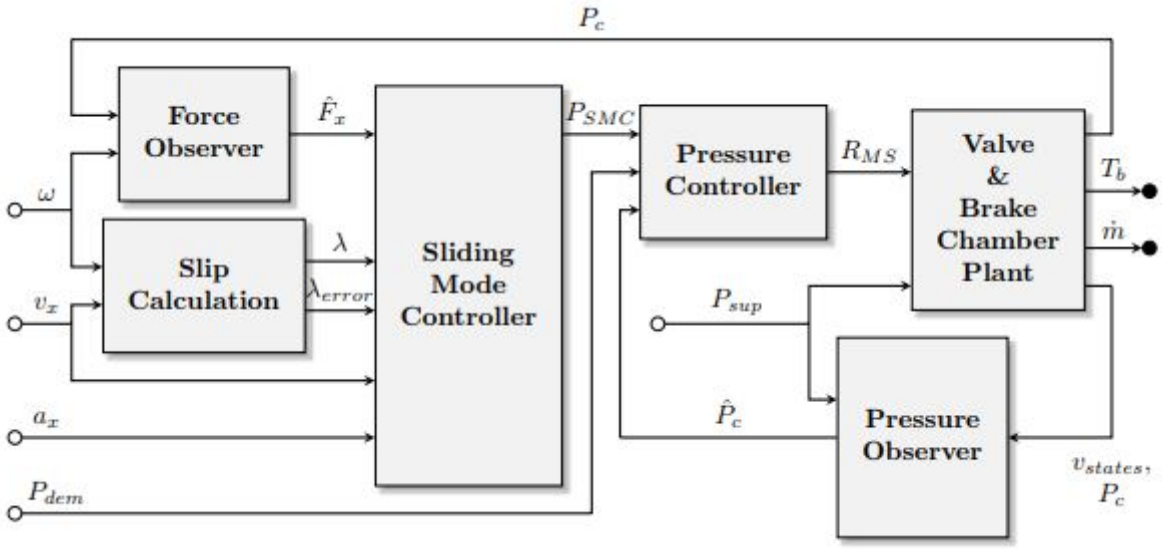

Figure 2.11: Schematic representation of the Actuators and Control Block [16]

The Sliding mode controller plays a pivotal part of the slip control braking. For the controller, a first order sliding surface is defined as:

$$s_s = \lambda - \lambda_{ref} \tag{2.17}$$

Where λ and λ_{ref} are the actual slip and reference slip.

The sliding mode controller determines the pressure which will then be used by pressure controller. The brake pressure can be given by:

$$P_{SMC} = \frac{R_r r_b \hat{F}_x - (1-\lambda) a_x J_\omega}{K_{BG} R_r} - k_s \frac{s_s}{s_s + \delta} - \Phi_s s_s \tag{2.18}$$

where R_r, K_{BG}, k_s, δ_s and Φ_s are the wheel rolling radius, brake gain and tune-able controller gains

The pressure controller then uses the demanded pressure from the sliding mode controller and converts it to Pulse Width Modulation (PWM) Mark Space Ratio demand using a proportional controller. The Mark Space Ratio is given by:

$$R_{MS} = k_{press}(P_{dem} - P_c) \tag{2.19}$$

The valve and brake chamber plant consists of valve states model, pnuematic valve model, brake chamber and actuator. The valve states model converts the PWM signal mark space ratio determines inlet and outlet valve states where zero corresponds to fully open and one corresponds to fully closed positions of the valves. The flow through the valve is modelled using one-dimensional fluid flow theory. The pneumatic valve model determines the mass flow rates which is then directly fed into the brake chamber model. The air within the brake chamber is modelled as a polytropic gas of the form $PV^\alpha = constant$. The brake chamber pressure is then given by:

$$\alpha_{in} \dot{m_{in}} - \alpha_{out} \dot{m_{in}} = \frac{V_c \dot{P_c}}{R T_c} + \frac{\alpha_c P_c \dot{V_c}}{R T_c} \tag{2.20}$$

where $\dot{m}$, V_c, R, T_c, α are the mass flow rate (subscripts 'in' and 'out' represents the inlet and outlet valve respectively), the chamber volume, specific gas constant for air, brake chamber temperature, ratio of specific heats respectively. The actuator then converts the determined chamber pressure to braking torque given by:

$$T_B = K_{BG} P_c \tag{2.21}$$

A detailed explanation for the valve and brake chamber plant can be found in [13].

As can be seen, the brake gain plays important role in the sliding mode controller and the valve plant. As already mentioned, an online estimation is vital. In thesis, a simulink based model in VTM will be developed to determine the brake gain in real time. The methodology adopted will be discussed in further chapters.

2.9 Vehicle Motion Management Architecture

Heavy Vehicle Motion Management (HVMM) Architecture [38] is a reference architecture that supports customer specific functional requirements (FR) and non-functional requirements (NFR) for several domains on architectural level. HVMM includes components with the logic to perform main cases such as Mission planning, execution, and tracking (PET) for the respective time horizons [38]. According to the architecture, HVMM sends requests to and gets information from the wheel brake actuators. The information from HVMM is then sent out to higher layer functions that serves as a lumped collection of all functions that control the vehicle on a higher abstraction level [39]. A reference HVVM architecture at Volvo GTT is as shown below:

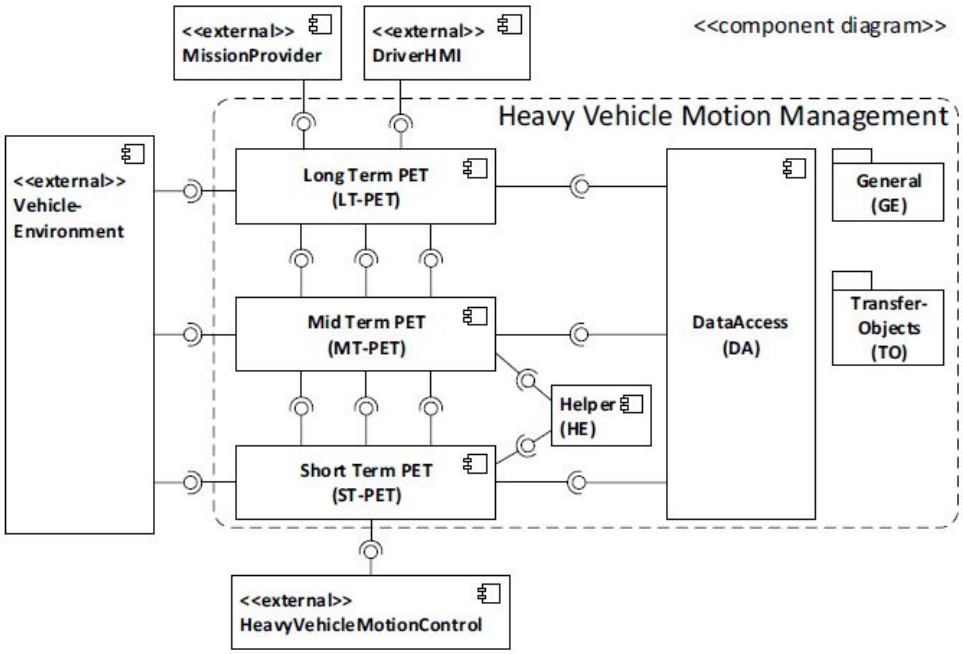

Figure 2.12: Heavy Vehicle Motion Management Architecture [38]

2.10 Brake Fade

Brake fade is one of the most common phenomenon resulting in poor braking. Brake fade can be defined as the loss of braking force/friction between the brake discs and pads. This is majorly due to excessive heat in the disc/pad system. Based on the cause, brake fade can be further divided into three categories:

- Mu Fade
  As the temperature increases the friction drops as the resistance of asperities to deform decreases. This will be discussed in depth in section 2.10.1
- Gas Fade
  Higher temperature in the disc/pad system causes deterioration of resin of

brake pad. The gases are trapped between the interface causing a decrease in frictional force.

- Water Fade
  In humid environment, water might get trapped in the interface causing reduced friction. Water fade is significant at higher speeds and low brake force which can be attributed to hydrodynamic effects of water films.

2.10.1 Mu(μ) Fade

The coefficient of friction between the disc and pad depends upon sliding speed, temperature and pressure where sliding speed is given by:

$$sliding\ speed = \frac{r_{br}}{R_r}\nu_x \tag{2.22}$$

Coefficient of friction(COF) with temperature varies as shown below:

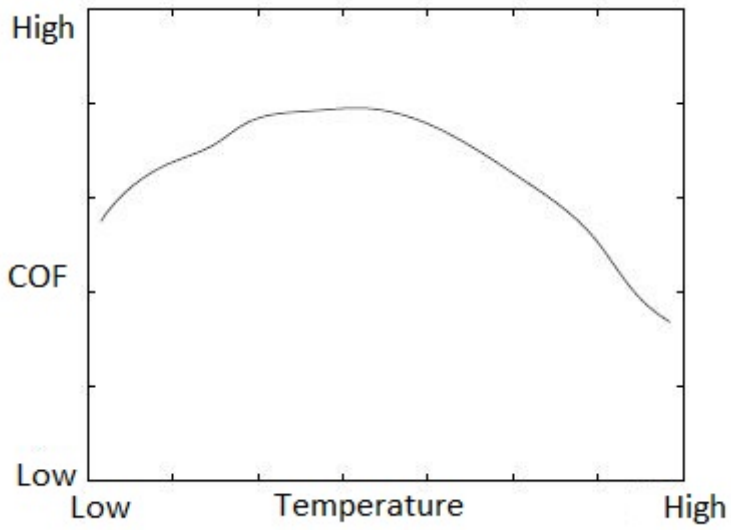

Figure 2.13: Variation of Coefficient of friction with Temperature [40]

Initially the coefficient of friction increases due to viscoelastic properties at elevated temperatures [41]. After this initial phase, the friction reaches a peak and then decreases as temperature increases. The decrease in friction coefficient can be attributed to thermal decomposition of the resin material of brake pad [42].

The coefficient of friction decreases with increase in sliding speed, see 4.3.2. This is due to lesser time available for asperities to come in contact and deform resulting in lower actual contact area.
As pressure increases, a large number of asperities come in contact with the disc increasing the contact area. This results in increase of the coefficient of friction with increase in pressure [43].

3
Methodology

3.1 Sensitivity Analysis

As shown in the section 2.8, the local brake controller uses the brake gain to determine the pressure demand. The valve and brake chamber plant uses pressure demand information along with the brake gain to determine the brake torque to be applied. To study the effect of brake gain change on the slip controller, a sensitivity analysis was performed. The brake gain varies up to 50% [12]. Hence, the extremes considered for the study are +50% and -50% of the predefined brake gain value.

The sensitivity analysis was performed in two stages:

- Sensitivity analysis 1: The brake gain included in the 'brake chamber plant' and the 'local brake controller' are varied equally.
- Sensitivity analysis 2: The brake gain of the local brake controller was varied but the valve and brake chamber plant gain was set to predefined value.

The analysis was realized in simulink and the following test matrices was adopted.

Table 3.1: Test matrix for Sensitivity Analysis 1

Test No.	Brake Gains	
	Local Brake Controller	Valve and Brake Chamber Plant
1	Predefined value	Predefined value
2	50% less than predefined value	50% less than predefined value
3	50% more than predefined value	50% more than predefined value

Table 3.2: Test Matrix for Sensitivity Analysis 2

Test No.	Brake Gains	
	Local Brake Controller	Valve and Brake Chamber Plant
1	50% less than predefined value	Predefined value
2	50% more than predefined value	Predefined value

3.2 Thermal Modelling of Brake System

Lumped parameter model is the most commonly used method to estimate disc temperature for continuous braking. The assumption made in lumped parameter model is that conduction of heat energy within the brake disc is higher than convection of heat energy from the disc to air flow. This assumption is validated using a dimensionless Biot number B_i [20]. A lumped parameter model of a disc is valid only if $B_i < 0.1$.

$$B_i = \frac{hr_0}{K} \tag{3.1}$$

Where, h, K, r_0 are convective heat transfer coefficient, conductive heat transfer coefficient and disc radius respectively.

The validation of our model was checked using h & K values from previous temperature estimation for drum brake [35] and the biot number was less than 0.1. An overview of Simulink model structure is as shown in the figure below:

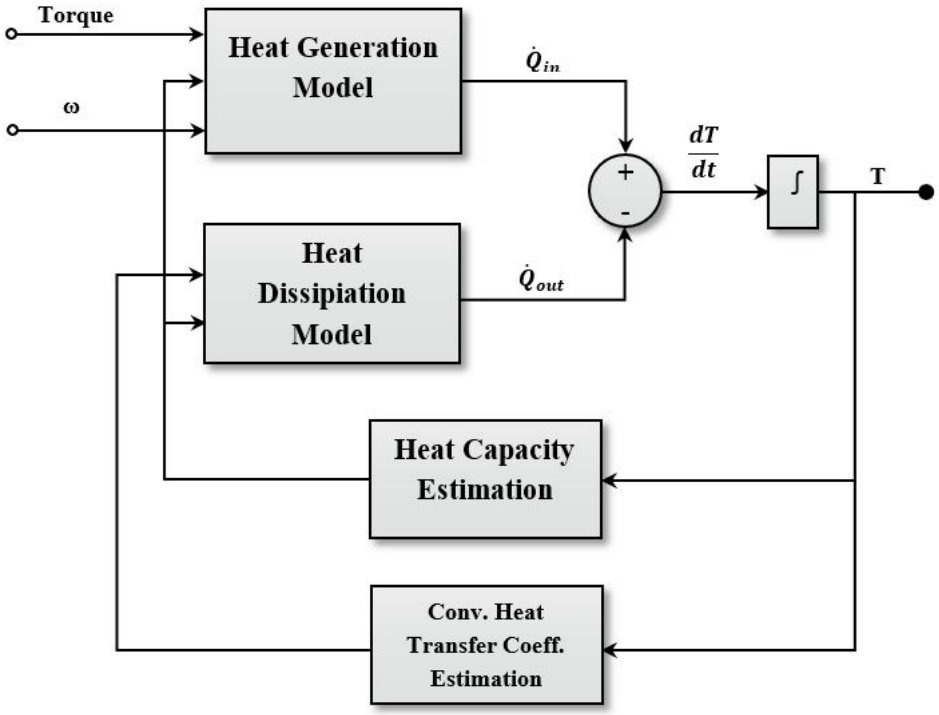

Figure 3.1: Thermal model

The heat generation is modelled using Eq.2.8. The inputs torque (or pressure) and velocity (wheel speed) are from VTM. In the heat dissipation model, the convection heat transfer is modelled using Eq.2.9. The heat generation and dissipation model is integrated according to Eq.2.6 to calculate the temperature.

3.2.1 Convective Heat Transfer Coefficient

The convective heat transfer h and active convective surface A_s are determined by parametreizing as 2.12. The convective heat transfer coefficient varies linearly with temperature and velocity. [34] derived an explicit relation between cooling coefficient, temperature and vehicle velocity using the test data:

$$b = b_0 + b_1 T + b_2 \nu_x \tag{3.2}$$

where b_0, b_1 & b_2 are constants that is determined from the test data.

3.2.1.1 Test Data

We know that the cooling coefficient depends on both temperature and velocity. In order to understand the cumulative effect of both, Volvo internal test data that includes different speed intervals and brake loads/Temperature was utilized. The tests involved driving the truck to a certain velocity range and braked intermittently to reach a specific temperature range. The combination of different speed and temperature intervals achieved is shown in the test matrix (Table 3.3). Once the required temperature was achieved, the truck was brought to a standstill (ν=0) and was allowed to cool down to ambient temperature. Since, ν becomes zero, these tests allow us determine the constants b_0 and b_1 using regression analysis.

Table 3.3: Test Matrix used to determine the cooling coefficient

	Speed (km/h)		
Temperature (deg C)	0-30	40-60	60-80
0-200	✓	✓	✓
250-350			✓
350-500			✓

The temperature was measured using sliding disc temperature sensors. In the case of 0-200 deg C tests, the velocity of the truck was maintained constant velocity for about an hour before coming to stand still. Again, for this range of data, regression analysis along with the known values of b_0 and b_1 was used to determine b_2.

3.2.2 Validation of Temperature estimation

The temperature estimation from the model was validated through a data set gathered from a truck which drove in and around London. The data set contained the brake pressure, velocity of the truck and brake disc temperature. The pressure and velocity was used as the input to the temperature estimator. A constant brake gain was assumed to simplify the validation. The simulation was performed for 40000 seconds and the predicted temperature was compared with the actual temperature.

3.3 Friction Estimation

As mentioned in section 2.5, the friction coefficient depends on various factors. Temperature and sliding velocity majorly contribute to the coefficient of friction. A direct measurement of coefficient of friction is not possible, however, if braking torque, applied pressure and mechanical design characteristics of the brake chamber is available, the coefficient of friction can be easily calculated using equation 2.3. Hence, in this case a dynamo-meter test was considered suitable.

3.3.1 Test Cycle

Out of available data sets from the dynamometer tests, temperature sensitivity test and speed sensitivity test were considered in our analysis.

In the temperature sensitivity tests, the brake disc is initially heated to various temperatures. Pressure range of 1-10 bar is applied for different initial vehicle speed and the brake torque is measured.

In the velocity sensitivity tests, the brake disc is initially heated to 100 deg C. Pressure range of 1-10 bar is applied for different initial vehicle speed and the brake torque is measured. The test matrix for two tests are as below:

Table 3.4: Temperature Sensitivity Test Matrix

	Speed (km/h)			
Temperature (deg C)	40	60	80	100
100	✓	✓	✓	✓
200	✓	✓	✓	✓
300	✓	✓	✓	✓
400	✓	✓	✓	✓
500	✓	✓	✓	✓
600	✓	✓	✓	✓

Table 3.5: Speed Sensitivity Test Matrix

	Speed (km/h)				
Temperature (deg C)	40	60	80	100	120
100	✓	✓	✓	✓	✓

3.3.2 Regression Analysis for Friction estimation

Matlab's inbuilt tool *cftool* was used for regression analysis. The sensitivity tests enabled to create mathematical model for temperature and velocity dependency. The models were then combined together to form a mathematical model for friction estimation.

3.4 Lever ratio estimation

As mentioned in the section 2.6, the stroke changes with chamber temperature and pressure. Though the stroke can measured using displacement sensors, not all the trucks can be equipped with it. So stroke is estimated using a mathematical model derived from available temperature sensitivity wear test data.

During the wear tests, the brakes are heated to desired temperature and brake pressure of $0-2.5$ bars is applied and the corresponding stroke length, temperatures and brake torques are measured. This test cycle is repeated for initial brake temperature range of $100-500°C$.

Using Matlab´s tool *cftool* for regression analysis a mathematical model is derived to estimate the stroke corresponding to the pressure applied and the brake temperature. The stroke values are used to determine the instantaneous lever length and hence the lever ratio is calculated. The block diagram of the Simulink model is as shown below:

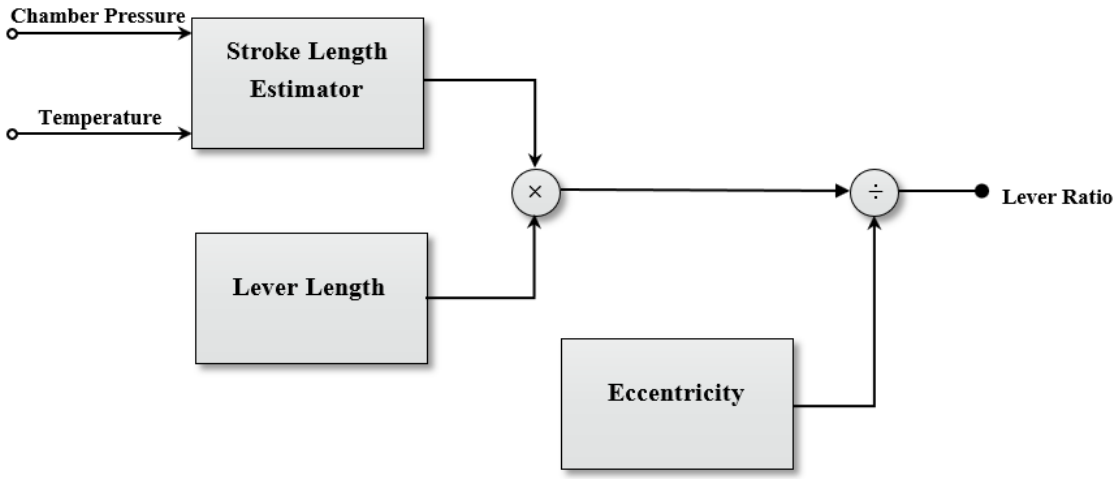

Figure 3.2: Lever ratio model

3.5 Brake Gain Estimation Routine

Using the estimated temperature, coefficient of friction and lever ratio in the following implemented simulink model, the brake gain can be estimated.

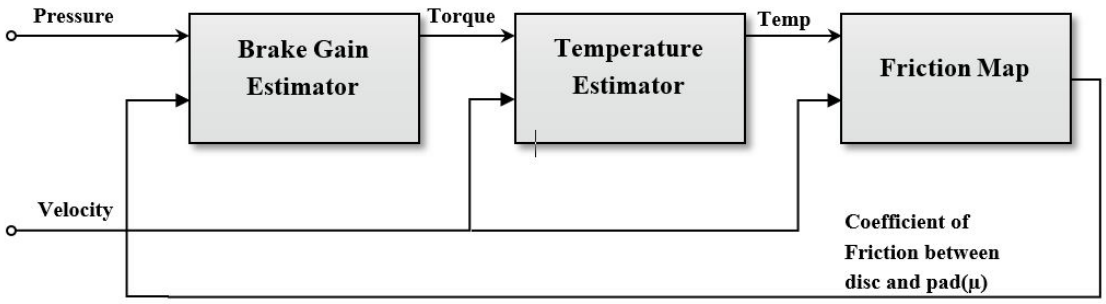

Figure 3.3: Block diagram representing the simulink model implementation

3.6 Brake Capability Estimator

Similar to batteries, brake disc can be considered as energy reservoirs. As braking event occurs, the brake discs heat up and the energy reservoir begins to become 'full'. The braking time available before the reservoir becomes 'full' can be termed as braking capability. This information can then be used by higher layers of VMM architecture for predicting brake fade and hence better speed profile planning.

From section 3.3, it was found that the coefficient of friction drops rapidly after 600 deg C. Hence for brake capability estimation, 600 deg C was considered the upper limit. Rewriting equation 2.6 and rearranging, we get:

$$t = c_p m_{disc} \frac{600 - T}{(\dot{Q}_{in} - \dot{Q}_{out})} \tag{3.3}$$

3.7 VTM Integration

The simulink based estimators was then integrated with the existing Volvo Transportation Model (VTM). The simulation test case adopted for the truck model was to brake with a initial velocity of 80 km/h with simulation time of 20 seconds. The simulation consisted of various braking and acceleration intervals. The major interest through this test was to study the performance of the developed estimators when integrated into the VTM environment.

4

Results

4.1 Sensitivity Analysis

4.1.1 Sensitivity Analysis 1

To study the overall effect of change in brake gain on the existing wheel slip controller sensitivity analysis-1 was performed. The behaviour of the wheel slip controller with default brake gain is as below:

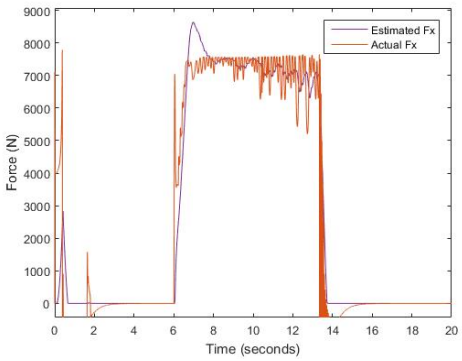

(a) Plot of estimated vs actual braking force

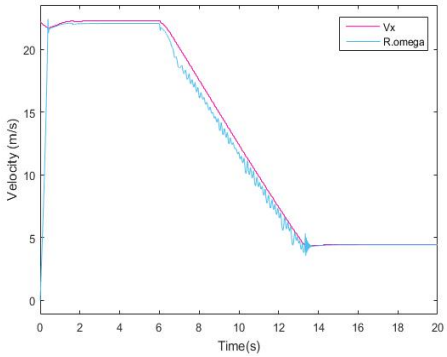

(b) Plot of ν_x and $R_r\omega$

Figure 4.1: Performance of the wheel slip controller with predefined brake gain

From the above graph, it can be observed that the prediction of braking force by brake controller is within tolerance. The behaviour of wheel slip controller with the modified brake gain values is as shown below:

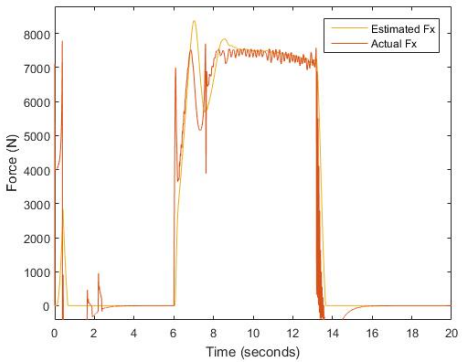

(a) Plot of estimated vs actual braking force

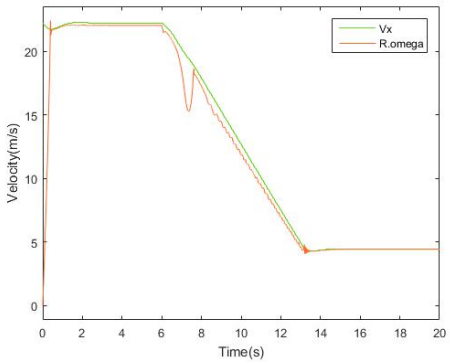

(b) Plot of ν_x and $R_r\omega$

Figure 4.2: Performance of the wheel slip controller with 50% decrease in brake gain

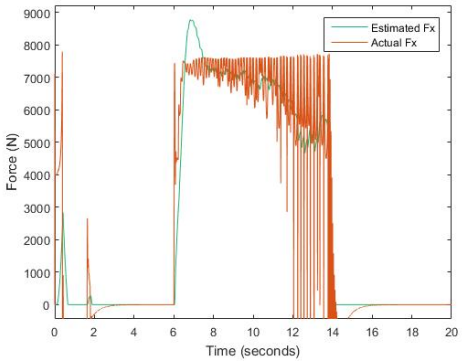

(a) Plot of estimated vs actual braking force

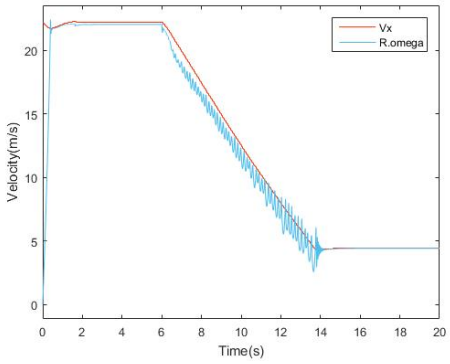

(b) Plot of ν_x and $R_r\omega$

Figure 4.3: Performance of the wheel slip controller with 50% increased brake gain

From the above graphs, it was observed that the braking force estimator works as expected in both the cases. However, as the brake gain increases, there is lot of disturbances present in the slip achieved. This is most likely due to the brake gain values selected for the slip controller during the sensitivity analysis being too high. On the contrary, the slip controller performed better when the gain was lowered.

4.1.2 Sensitivity Analysis 2

To study the effect of different brake gain values in the brake controller and the valve plant on the performance of wheel slip controller sensitivity analysis-2 was performed. The behaviour of wheel slip controller with different brake gain values in the brake controller and valve plant is as shown below:

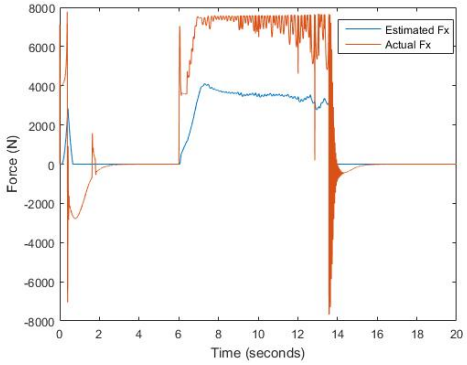

(a) Plot of estimated vs actual braking force

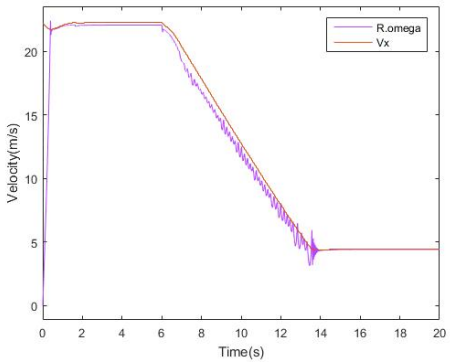

(b) Plot of ν_x and $R_r\omega$

Figure 4.4: Performance of the wheel slip controller with 50% decrease in brake gain of the brake controller

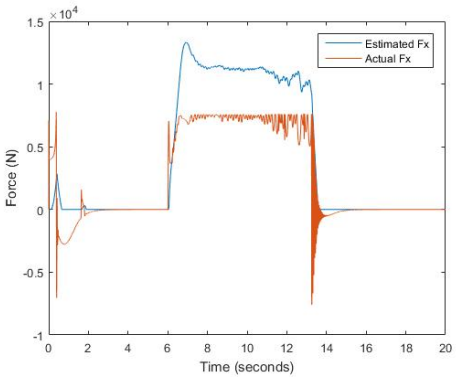

(a) Plot of estimated vs actual braking force

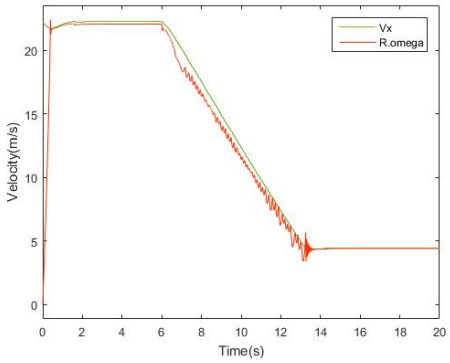

(b) Plot of ν_x and $R_r\omega$

Figure 4.5: Performance of the wheel slip controller with 50% increased brake gain of the brake controller

From the graphs above, it is observed that in both cases the estimated braking force is not equal to the actual braking force. The estimated F_x is used to determine the coefficient of friction between tyre and the road and the error in estimation would clearly corrupt the friction estimation. It is also noted that the estimated and actual braking forces are much lower compared to figure 4.1b. When the brake gain is decreased by 50%, the brake controller determines lower pressure demand since the controller predicts a lower available braking force. This results in a lower braking torque and the braking distance increased by 5 meters. The same explanation holds true for when the brake gain is increased. The wheel slip also showed large disturbances in both the cases as can be seen in figure 4.4b and 4.5b.

4.2 Temperature Model

4.2.1 Convective Heat Transfer

As mentioned in the section 3.2.1.1 using the available vehicle test data, the regression analysis of the cooling curves is performed to determine the values of b_0, b_1 and b_2 for the test matrix 3.3. The results from the regression analysis for different initial temperature are as shown in the figures below and curve fitted to determine b_0 & b_1 values.

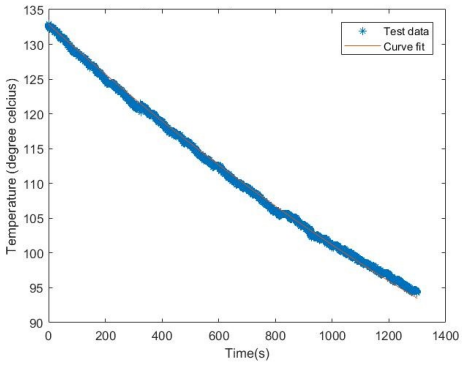

(a) Regression Analysis for 100-200 deg C & 60-80 Kmph

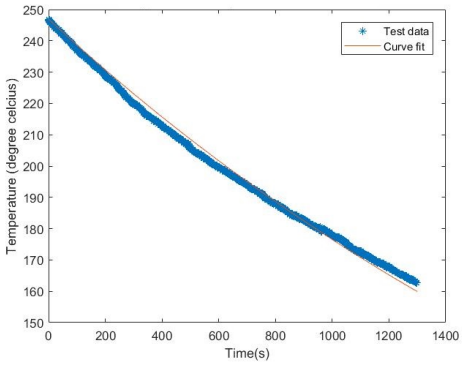

(b) Regression Analysis for 0-200 deg C & 0-60 Kmph

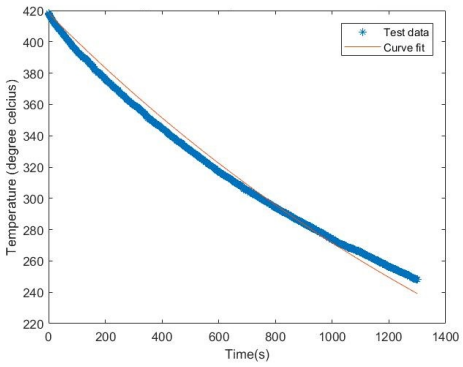

(c) Regression Analysis for 0-200 deg C & 60-80 Kmph

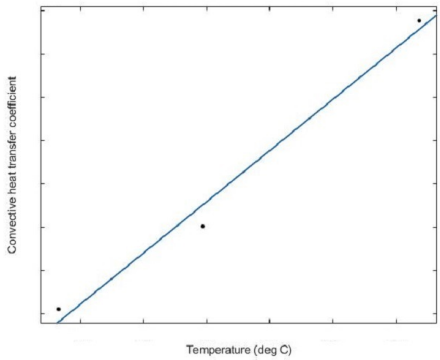

(d) b_0&b_1 fit

Figure 4.6: Regression analysis to determine b_0 and b_1

Using the temperature dependent b_0 & b_1 values, the curve fit for constant temperature $200°C$ and brake velocity $0-30, 40-60$ & $60-80$s the mean velocity dependent b_2 value is determined. The results of the regression analysis and curve fit for b_2 is as shown below:

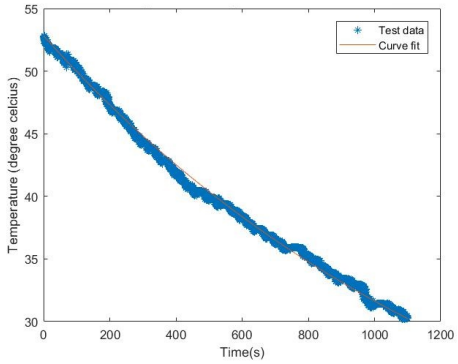

(a) Regression Analysis for 0-200 deg C & 60-80 Kmph

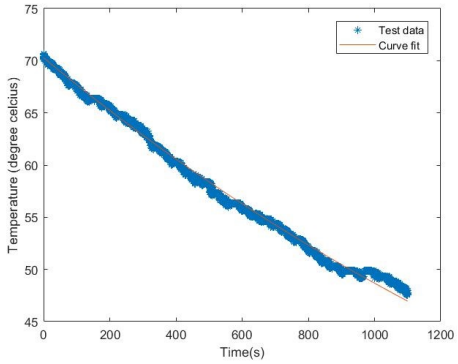

(b) Regression Analysis for 0-200 deg C & 0-60 Kmph

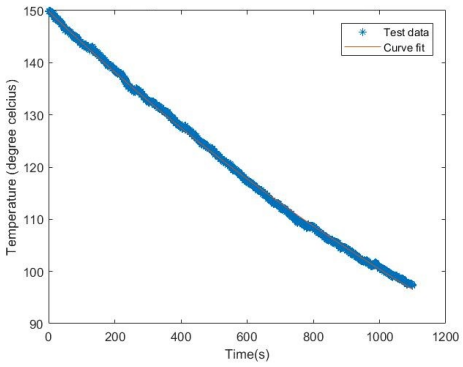

(c) Regression Analysis for 0-200 deg C & 0-30 Kmph

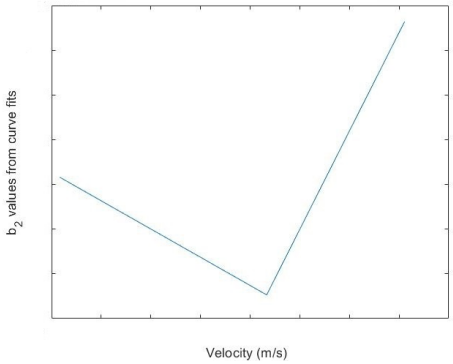

(d) Mean b_2 value for 0-200 deg C & different velocities

Figure 4.7: Regression analysis to determine b_2

The determined cooling co-coefficients constants are tabulated in Appendix A.

4.2.2 Temperature Validation

To validate the temperature estimation model, test data of a disc braked garbage truck is used. The test was conducted in London. The performance of the estimator is as expected and the result is as shown in Figure 4.8. Red line indicating the estimated temperature and blue line the measured value. The glitches from the measured values is due to sensor error.

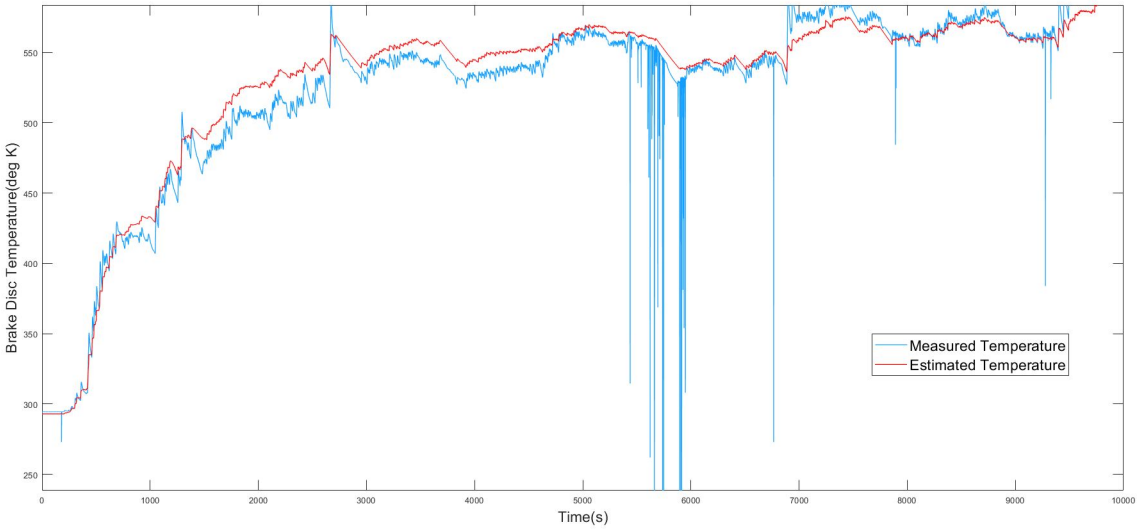

Figure 4.8: Estimated temperature and measured temperature data of a garbage truck

.

4.3 Friction Estimation

4.3.1 Variation of friction with temperature

Based on the Volvo dynamometer test data, the coefficient of friction was plotted for various temperatures as shown below:

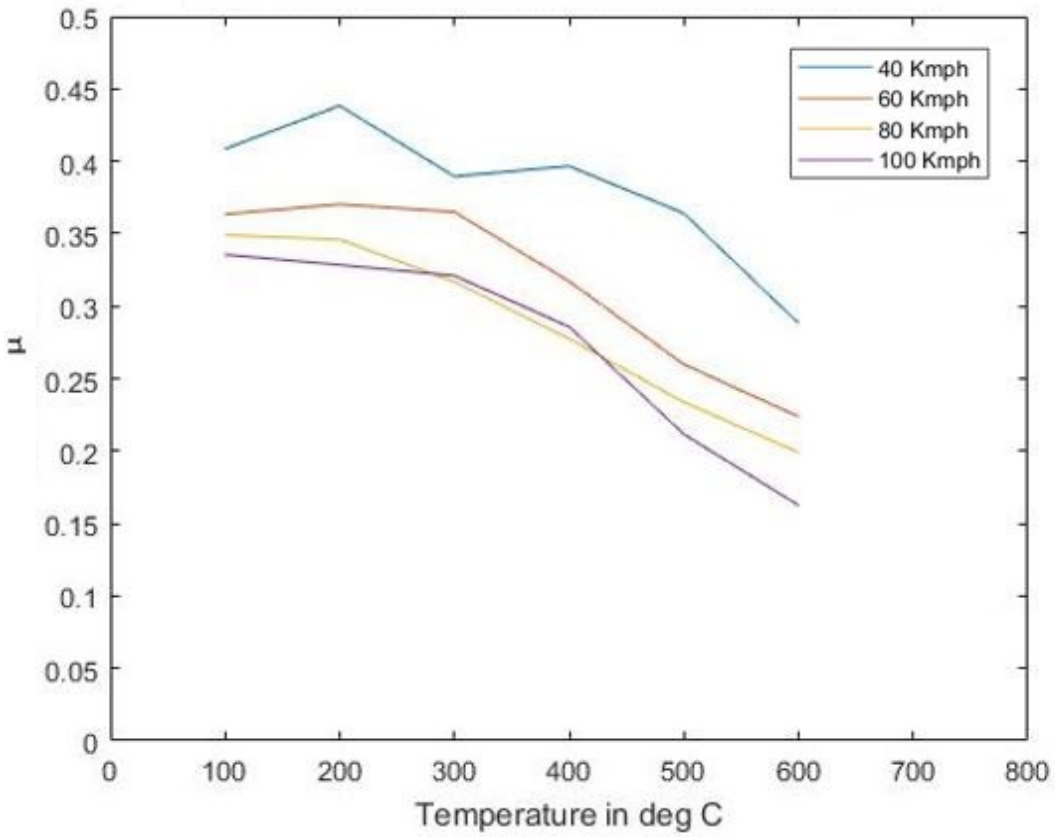

Figure 4.9: Plot of COF with respect to temperature for various initial sliding speeds

4.3.2 Variation of friction with speed

The COF plotted for various velocities as shown in below based on test data.

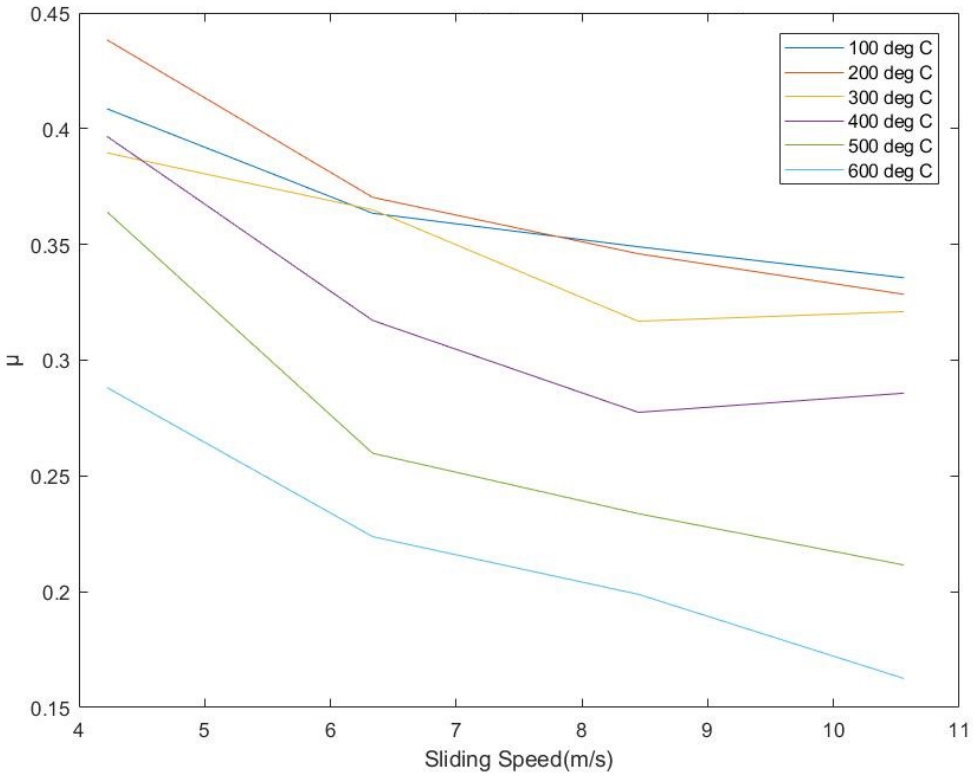

Figure 4.10: Plot of COF with respect to sliding speed for various initial temperature

4.3.3 Combined Friction Model

It can be seen that the COF has a logarithmic decrease with respect to velocity. However, with temperature, the COF remains constant initially and decreases as temperature increases further. Iterations of regression analysis showed that a polynomial fit was able to capture the information well in the temperature zone. The mathematical model capturing the effects of velocity and temperature is as below:

$$\mu(T, v) = (a_1 T^2 + a_2 T) + b_1 (b_2)^v \tag{4.1}$$

where, a_1,a_2,b_1 and b_2 are constants, μ,T and v are coefficient of friction, temperature(in deg C) and sliding velocity(in m/s) respectively. The developed friction model is not intended to use outside 4<v<10 m/s and 100<T<600 deg C.

The fit above mathematical model to the test data and residual/error is as below:

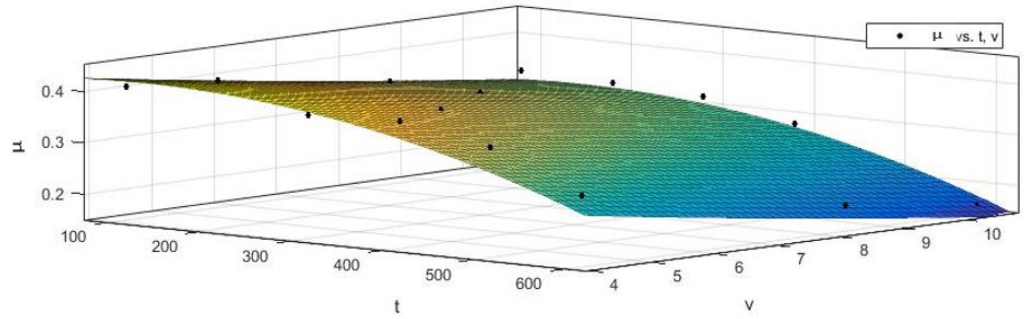

Figure 4.11: Best fit of mathematical model to the test data

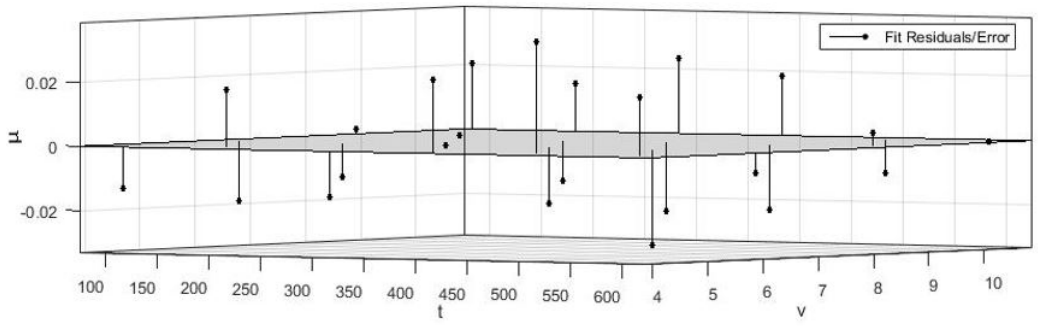

Figure 4.12: Best fit residuals

It can be seen that the generated error is less than 0.4%, hence the model is acceptable. The values of the constants determined are tabulated in appendix A.

4.4 Effect of Lever ratio

The derived mathematical model from the highest (500°) Haldex actuator temperature test data is as follows:

$$SL(T, P) = a_0 + a_1T + a_2P + a_3T^2 + a_4PT + a_5P^2 \tag{4.2}$$

Where SL is the stroke length, P is the brake pressure,T is the temperature and $a_0, a_1, a_2, a_3, a_4, a_5$ are the coefficients.
The estimation model is verified for different initial braking temperature test data from Haldex and results of the estimation in as shown in Figure 4.14. The lever ratio change with temperature, pressure is as shown in Figure 4.15.

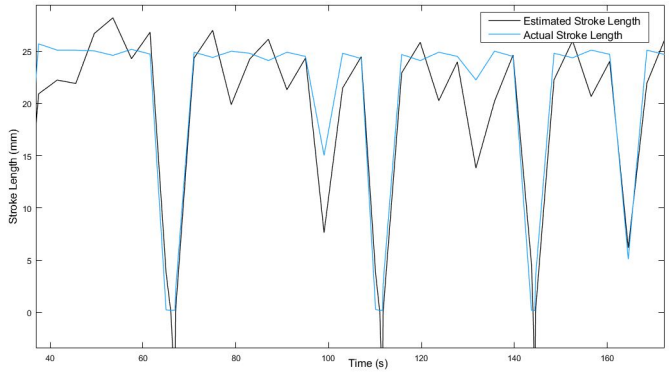

Figure 4.13: Stroke Length vs Time for braking temperature 400°C

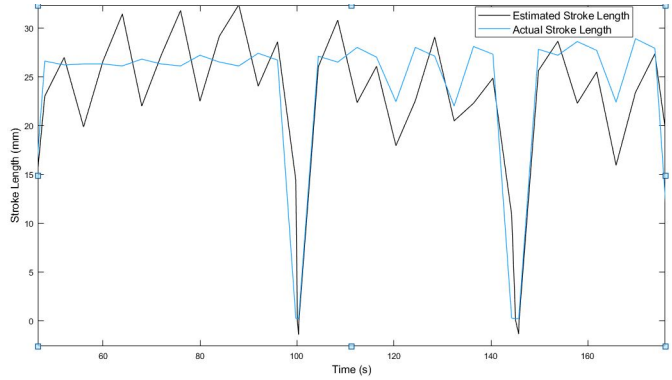

Figure 4.14: Stroke Length vs Time for braking temperature 500°C

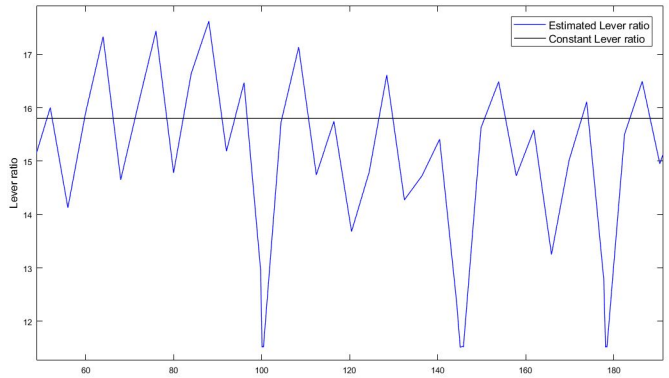

Figure 4.15: Lever ratio change at 500°C

The brake gain value using the estimated lever ratio is compared with the brake gain with constant lever ratio '15.8' [45] as shown in Figure 4.16. The difference between the brake gain values are as shown in the Figure 4.17.

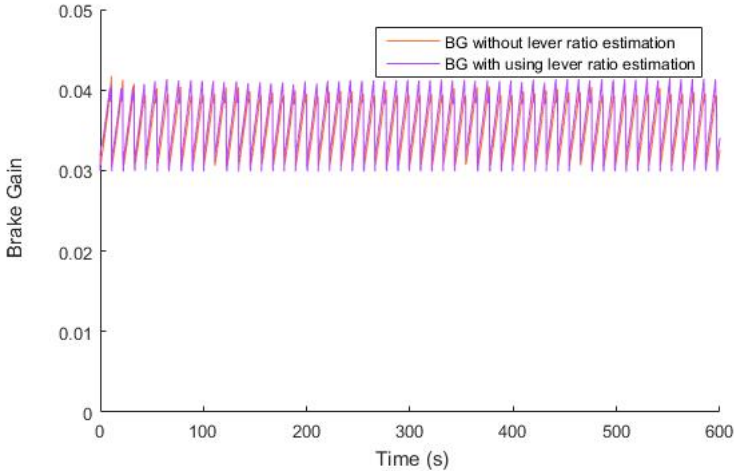

Figure 4.16: The effect of lever ratio on brake gain(fixed)

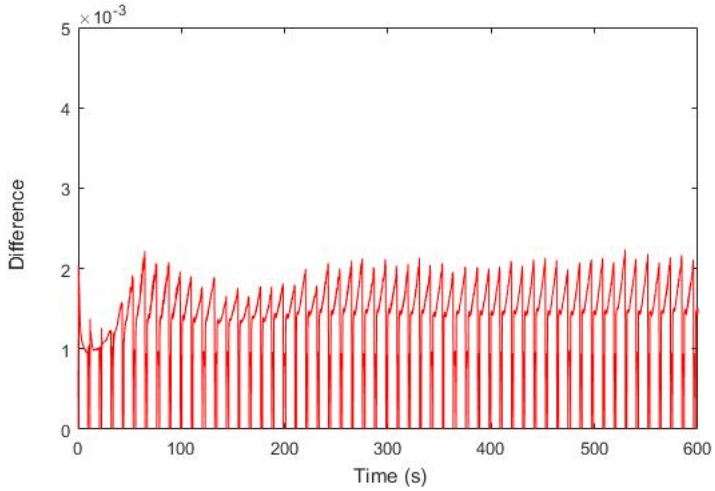

Figure 4.17: The difference in brake gain values

4.5 Brake Gain Comparison

To study the robustness and to validate the brake gain estimator, the test data from Haldex dynamometer was used. The temperature range was 100-500 deg C and velocity range of 40-100 kmph. The test involved heating the brake disc to the required temperature followed by accelerating the disc to 100kmph. Brakes were then applied until the disc reached the lower velocity i.e 40 kmph and the cycle was repeated several times. Temperature, velocities, pressure applied and brake torque generated by the brakes were measured throughout the test. For initial temperature of 100 deg C, velocity range of 10-60 kmph was chosen. This provides the ideal platform to study the estimator robustness. However, the Haldex system differs from the volvo brake system in terms of the type of disc, the brake pad composition and caliper mechanism. The following brake gains were compared:

- Actual Brake Gain- The ratio of the torque generated and pressure applied directly provides the actual brake gain.

- Constant Brake Gain- The 'assumed' constant brake gain currently being used at Volvo.
- Estimated Brake Gain- The temperature and velocity values from the dynamometer was fed to the brake gain estimator to determine the brake gain.

The comparison is as below:

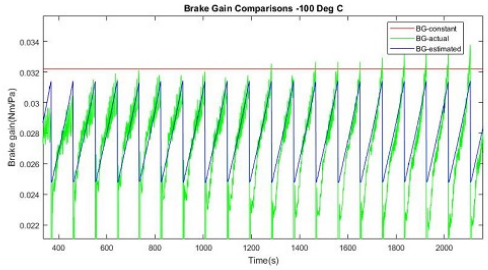

(a) Brake gain comparison at 100 deg C

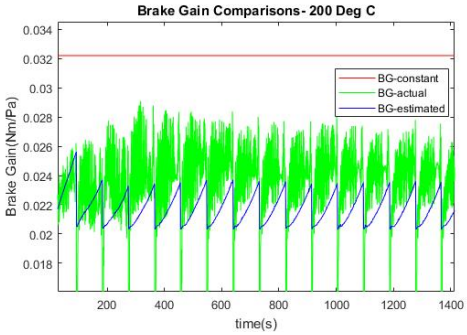

(b) Brake gain comparison at 200 deg C

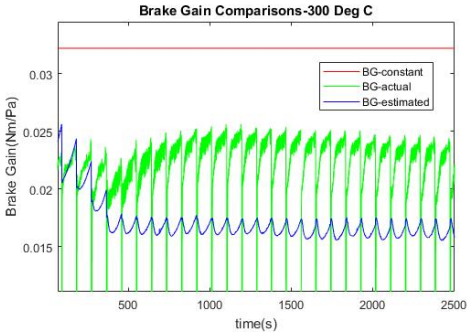

(c) Brake gain comparison at 300 deg C

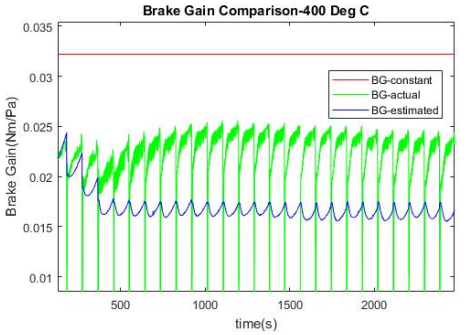

(d) Brake gain comparison at 400 deg C

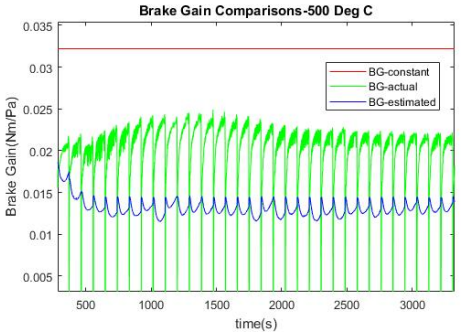

(e) Brake gain comparison at 500 deg C

Figure 4.18: Actual, constant and estimated brake gain comparisons

4.6 VTM Integration

Temperature, Coefficient of friction and the brake capability were of the most interest when integrated into VTM. The results for front left wheel through this simulation is shown below:

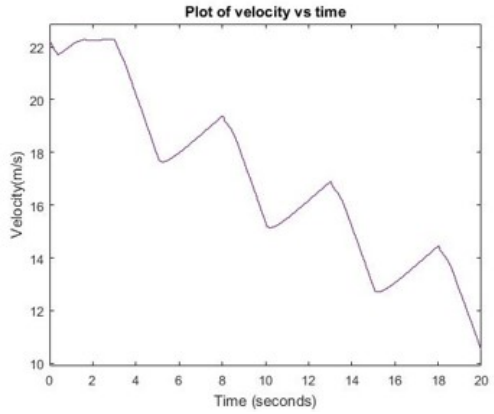

(a) Plot of velocity with time

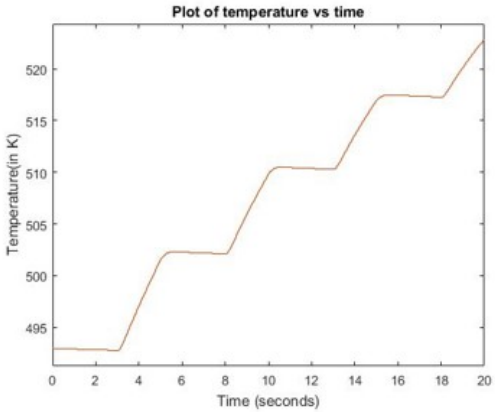

(b) Plot of temperature with time

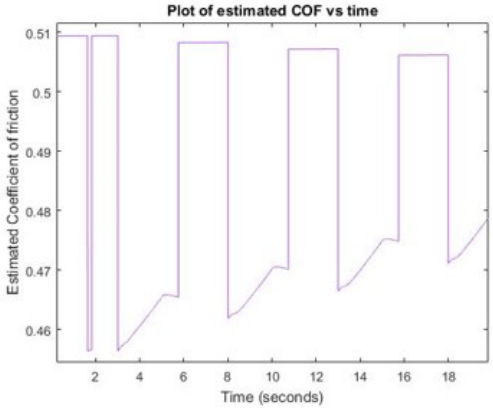

(c) Plot of coefficeint of friction with time

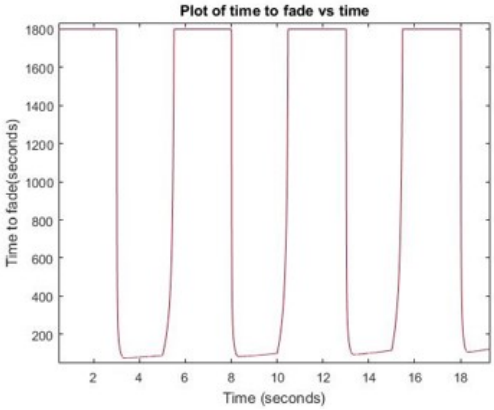

(d) Plot of time to fade with time

Figure 4.19: Performance of estimators integrated with VTM

5
Discussion

5.1 Sensitvity Analysis

The sensitivity analysis presents that the variation in the brake gain can severely affect the performance of the wheel slip controller. Also, as expected, the simulations showed an increase in braking distance with decrease in brake gain. Section 4.1.1 shows that a decrease in the brake gain affects the performance of the controller positively whereas a increase in the brake gain affects the performance negatively. However, a difference (positive or negative) in the brake gain between the local brake controller and Valve and brake chamber plant affects the performance negatively as shown in section 4.1.2. This further establishes a clear motivation to estimate brake gain in real time in order to have a better functioning of brake system controller.

5.2 Thermal Modelling

5.2.1 Cooling coefficient estimation

From the available cooling data, the b_0, b_1 & $b2$ values are derived through curve fit for different cooling temperature and at different brake velocity. The cooling coefficient estimation model includes both temperature and velocity influence. However the cooling of the disc depends on a lot of different parameters such as ambient temperature, wind velocity, aerodynamics of the vehicle, etc. This makes it hard to derive a model that takes into account the randomness of driving in different weather conditions.

5.2.2 Temperature Estimation

The temperature estimation model seems to function as expected. The results from the model is validated against the available truck data and the maximum error in the estimation is around $20°C$. This error might be due to the simplified cooling model. The model is setup at different weather condition that results in estimating a higher temperature and this continues. But at higher temperature (>700 deg C), the estimation fails to converge with the sudden measured peak. This may depend on the simplified modeling of the bulk temperature as a uniform temperature. However more test data is desired to validate the estimation model. In the available truck data, the temperature was measured using two thermo-couples one on inner and outer disc surface. The temperature estimation is validated against the

mean temperature value. Since we follow lumped capacitance method, for better mean temperature value using higher number of thermo-couples for measurement is desired.

5.3 Friction Estimation

From figure 4.9 and 4.10, it can be seen that as expected the coefficient of friction decreases with increase in temperature and sliding velocity. The combined effect of temperature and velocity is also evident. A pattern for the coefficient of friction decrease was observed in both cases. This enables us to clearly establish a mathematical model to predict the friction behaviour. The proposed friction model performs very well in the temperature range (100-600 deg C) and sliding velocity range (4-11 m/s) with error (<0.4%) as can been seen from figure 4.12. However, due to lack of test data at low temperature (<100 deg C) or high temperature (>600 deg C), the estimation results have not been validated in these temperature ranges. Based on various literature studies, the authors expect the mathematical model to predict accurately well in those ranges as well.

5.4 Lever Ratio Estimation

From the comparison in the section 4.4, the difference in brake gain values using the lever ratio estimation and constant lever ratio is as shown in the Figure 4.16. The effect of lever ratio is also validated using the available dynotest data by back calculating the brake gain from brake torque and chamber pressure with mechanical efficiency of 95%. The lever ratio model predicts that the effective lever ratio can reduce the brake gain by up to 5% for brake temperature above $500°C$

5.5 Brake Gain

When the brake gain comparison was performed for the two different brake disc/pad (Volvo inhouse and Haldex) combination, the estimation predicts accurately for lower temperature ranges such as 100 and 200 deg C as seen in figure 4.18a and 4.18b. However, as the temperature increases to 300-500 deg C, the estimation clearly underestimates as seen in 4.18c, 4.18d and 4.18e. It can be noted that the error in estimation increases from 4.18c to 4.18e. The reason is that the decrease in the friction coefficient is much lower than estimated. This shows that the performance varies for different brake disc/pad combination.

5.6 Brake Capability

Depending on the information demanded by the higher layers in the VMM architecture, the brake capability estimator can be modified to estimate available energy or time before brake fade occurs to help in path and velocity planning. In this thesis, time to brake fade was considered sufficient at each braking event. The brake

capability estimator performed as expected when integrated with the temperature estimator.

5.7 VTM Integration

The estimators performed well when integrated with VTM. The temperature increases as expected during the braking event as can be seen from 4.19b. After the braking event at 14 seconds, the temperature begins to decrease. Since the cooling happens for 6 seconds and the velocity of the truck is so low, the decrease is unnoticeable. The coefficient increases at the braking event due to phenomenon already explained in section 2.10.1. The brake capability estimator predicts the brake to fade at approximately 132 seconds if the brake event continues in similar fashion. However due to noise, large values creep in during the non-braking phase, causing the brake fade time to be unrecognizable during the braking phase.

6
Conclusion

The 'brake gain' is estimated through the temperature and friction coefficient between the disc and the pad. The developed temperature and friction models does justice in predicting the temperature and friction respectively. Although a braking event is defined as reducing a vehicle speed by converting kinetic energy to heat energy through friction between brake disc and pad, a complicated set of events occur at the pad surface. Major reasons include the material composition and structure of the brake pad. Also, since the asperities formation and development of the brake pad varies depending on braking history and usage, coefficient of friction differs between brake pads. In order to completely capture these effects the friction model requires on-line calibration. The temperature and friction model in this thesis work are simple and can be easily implemented in a real truck. However, the parameters in the models needs to be tuned in order to adapt the existing models to other brake disc/pad combination. The change in lever ratio of the brake mechanism due to temperature and chamber pressure has negligible effect on brake gain. Hence lever ratio can be considered to be constant.

The brake capability estimator is dependent on the temperature estimation. Hence an improved temperature estimator can improve the performance of the brake capability estimator.

Bibliography

[1] CED technologies. *http://www.cedtechnologies.com/heavy-truck-braking/*, 2011.

[2] European Road Safety Observatory(ERSO). *Traffic Safety Basic Facts*, 2017

[3] Volvo Trucks Accident Research Team. Volvo Trucks Safety Report,2017.

[4] Bendix.*https://www.cbsparts.ca/admin/bulletins/SD-23-7541$_U$S$_0$03%20rfs.pdf*

[5] Ernst Göhring, Egon-Christian von Glasner, and Rolf Povel, Engine Braking Systems and Retarders - An Overview from an European Standpoint,1992.

[6] National Highway Traffic Safety Administration. The Effectiveness of ABS in Heavy Truck Tractors and Trailers, 2010.

[7] Gillespie, T. 1992. Fundamentals of Vehicle Dynamics. s.l. : Society of Automotive Engineers, 1992.

[8] Bengt Jacobson. Vehicle Dynamics Compendium,2017.

[9] WABCO.*http://www.wabco-auto.com/en/products/category-type/brake-stability-control/advanced-braking-systems/electronic-braking-system-ebs/*

[10] Knorr-Bremse Group. *https://www.knorr-bremsesfn.biz/WCMS/Artpics/126/Bildart/Drawings/W1QhFAQpI0EBhB$_Y$074812$_{1E}$N$_0$03.pdf*

[11] J. Wrede and H. Decker. Brake by wire for commercial vehicles,In *Transactions of the SAE, pp. 849-859*, 1992.

[12] Jonathan I Miller. Advanced Braking Systems For Heavy Vehicles, 2010

[13] Leon M Henderson. Improving Emergency Braking Performance Of Heavy Goods Vehicles, 2013.

[14] Chankyu Lee, Karl Hedrick, and Kyongsu Yi. Real-Time Slip-Based Estimation of Maximum Tire–Road Friction Coefficient, In *IEEE/ASME Transactions of Mechatronics, VOL. 9, NO. 2*, 2004.

[15] Fredrik Granqvist, Carl-Johan Rundqvist. Estimation of disc brake performance using emperical modelling. 2005

[16] Bernhard Westerhof, Dimitrios Kalakos. Heavy Vehicle Braking using Friction Estimation for Controller Optimization, 2017.

[17] Faramarz Talati & Salman Jalalifar. Analysis of heat conduction in a disc brake system, In *Springer-Verlag*, 2009.

[18] Pyung Hwang, Xuan Wu and YoungBae Jeon,Yeungnam University. Repeated Brake Temperature Analysis of Ventilated Brake Disc on the Downhill Road, In *SAE TECHNICAL PAPER SERIES*,2008.

[19] Limpert, Cooling analysis of disc brake rotors. *SAE Technical Paper 971014*, 1975.

[20] L. Nisonger, Chih-hung Yen and David Antanaitis. High Temperature Brake Cooling - Characterization for Brake System Modeling in Race Track and High

Energy Driving Conditions Robert, In *SAE International doi:10.4271/2011-01-0566*,2011.

[21] H Sakamoto. Heat convection and design of brake discs, In *F01803 IMechE*, 2004.

[22] Kwangjin Lee,Delphi Automotive Systems. Numerical Prediction of Brake Fluid Temperature Rise During Braking and Heat Soaking, In *SAE Technical Paper series*, 1999.

[23] Shaoyang Zhang, Weiping Chen and Yuanyuan Li. Wear of Friction Material during Vehicle Braking,South China University of Technology. In, *SAE Technical Paper series*,2009.

[24] S. K. Rhee. Wear Mechanisms for Asbestos-Reinforced Automotive Friction Materials, In *Science direct,Wear,Volume 29, Issue 3, Pages 391-393*,September 1974.

[25] Limpert, R. Brake Design and Safety, 3rd Edition, In *SAE International*,2011.

[26] Jiusheng Bao,Yan Yin,Lijian Lu and Tonggang Liu. Tribological characterization on friction brake in continuous braking. In, *Industrial Lubrication and Tribology 70/1 (2018) 172–181*, 2018

[27] Ch.Hohmann, K.Schiffner & J.Brecht. Pas Wear Simulation Model. In, *SAE Technical Paper series*,1999.

[28] Todorovi J., Duboka ., Arseni Ž. Operational Life Expectancy of Rubbing Elements in Automotive Brakes. Tribology International, 28(7), 1995.

[29] Nagesh S.N,Siddaraju C,S V Prakash & M R Ramesh. Characterization if brake pads by variation in composition of friction materials. International Conference on Advances in Manufacturing and Materials Engineering, AMME 2014.

[30] David C. Sheridan, James A. Kutchey, and Farzad Samie. Approaches to the Thermal Modeling of Disc Brakes. Power Systems Research Dept. General Motors Research Laboratories Warren, MI. In, *SAE Technical Paper series*,1988.

[31] Schopper, A. Thermophysical Properties of 2 Metal Samples. Tech. rep. Applications Laboratory Thermophysical Properties Section, 2008.

[32] Kwangjin, L. Numerical prediction of brake fluid temperature rise during braking and heat soaking. *SAE Technical Paper 1999010483*,1999.

[33] Tirovic, M. Thermal effects in brakes, Braking of Road Vehicles 2013. University of Bradford. ISBN 978 1 85143 269 1,2013.

[34] Engineering report, Volvo GTT (ER-214915).

[35] Volvo GTT internal temperature estimation carried out for drum brakes, Martin Pettresson,Volvo GTT.

[36] Incropera, F. P. Introduction to Heat Transfer, 4th Edition. Wiley, 2001.

[37] M J Nunney, Light and Heavy vehicle Technology Introduction, 4th Edition, 2007.

[38] Jan Schroeder, Daniela Holzner, Christian Berger, Carl-Johan Hoel, Leo Laine and Anders Magnusson. Design and Evaluation of a Customizable Multi-Domain Reference Architecture on top of Product Lines of Self-Driving Heavy Vehicles – An Industrial Case Study,2015 IEEE/ACM 37th IEEE International Conference on Software Engineering.

[39] Kristoffer Tagesson, Driver-Centred Motion Control of Heavy Trucks, 2017.

[40] Asim Rashid, Overview of Disc Brakes and Related Phenomena - a review, 2014, International Journal of Vehicle Noise and Vibration, 10(4), pp. 257-301.
[41] U.S. Hong, S.L. Jung, K.H. Cho, M.H. Cho, S.J. Kim, and H. Jang. Wear mechanism of multiphase friction materials with different phenolic resin matrices. Wear, 266(7-8):739 – 744, 2009.
[42] W. Österle and A.I. Dmitriev. Functionality of conventional brake friction materials - perceptions from findings observed at different length scales. Wear, 271(9-10):2198–2207, 2011.
[43] M. Nosonovsky and B. Bhushan. Multiscale friction mechanisms and hierarchical surfaces in nano- and bio-tribology. Materials Science and Engineering: R: Reports, 58(3-5):162 – 193, 2007.
[44] Lars Svensson, Volvo internal report ER-669108, 2015.
[45] Haldex service Manual,DISC BRAKE ModulX DB22, DB22LT, DB19.
[46] Kristoffer Tagesson. Driver-centred Motion Control of Heavy Trucks, 2017

A

Appendix

A.1 Model Parameters

Values available in the Volvo version of the report

A.2 Cooling Coefficients

Values available in the Volvo version of the report

A.3 Friction model parameters

Values available in the Volvo version of the report

A.4 Lever ratio

Values available in the Volvo version of the report